DAMAGE EVOLUTION IN COMPOSITE MATERIALS UNDER ENVIRONMENTAL AGEING: A STOCHASTIC MODEL WITH EXPERIMENTAL VALIDATION

by

REZWANUR RAHMAN

A THESIS

Submitted in partial fulfillment of the requirements for
the degree of Master of Science in the Department
of Aerospace Engineering and Mechanics
in the Graduate School of
The University of Alabama

TUSCALOOSA, ALABAMA

2009

ABSTRACT

This work emphasizes on predicting probability density function of damages or "number density of damage" in graphite/epoxy polymer matrix composite materials (PMC) under hygrothermal aging condition. A coupled Forward-Backward Stochastic Differential Equation (FBSDE) is proposed as a mathematical model to predict number density of damages. The FBSDE consists of damage nucleation and annihilation rate in terms of Brownian motion. The uncertainty in damage nucleation and annihilation rate is noticed by proposing these two terms as "Brownian motion with drift".

In order to verify the proposed model, a quantitative analysis was carried out on a limited number of graphite/epoxy specimens manufactured by VARTM process. The specimens were kept in a hygrothermal condition with room temperature cycling. A rigorous quantitative analysis of damages was done by optical microscopic inspection at different stages of aging period. The damages were classified based on the criteria of their size.

Finally, the experimentally collected data for number density of damages were verified by using the proposed FBSDE. A detail parametric study was carried out using FBSDE and best possible predicted data was validated with the experimental observation. A reasonable estimation was observed from the model output.

DEDICATION

This thesis is dedicated to everyone who helped me and guided me through the trials and tribulations of creating this manuscript. In particular, my family and close friends who stood by me throughout the time taken to complete this masterpiece.

LIST OF ABBREVIATIONS AND SYMBOLS

x_i	Spatial coordinates
c	Damage size
ξ	Damage orientation
μ	Moisture concentration
h	Hardness
Φ	Temperature distribution
$[0,T]$	Overall time interval
$\left[0,T^*\right]$	Sub-interval of time
n_N	Nucleation rate
n_A	Annihilation rate
n	Number density of damages
$\{n_{N_t} : t \geq 0\}$	Nucleation rate as stochastic process
$\{n_{A_t} : t \geq 0\}$	Annihilation rate as stochastic process
ω	Probability state
B_t	Standard Brownian motion in any probability state (ω)
FSDE	Forward stochastic differential equation
BSDE	Backward stochastic differential equation

FBSDE	Backward-Forward stochastic differential equation
n_t	Number density of damages in terms of Brownian motion (Solution FSDE)
$\overline{n_t}$	Number density of damages in terms of Brownian motion (Solution BSDE)
$\underline{n}_t$	Number density of damages as predictable process (i.e. experimental observation)
N_t	Weighted average of solutions from BSDE ($\overline{n_t}$), FSDE (n_t) and the predictable process ($\underline{n}_t$)
β	Volatility of the Brownian motion (in FSDE)
σ	Volatility of the Brownian motion (in BSDE)
n_{t_0}	Initial condition for the FSDE
$\underline{n}_T$	Terminal condition for the BSDE
l_e	Total number of iterations
Δt	Incremental size
VARTM	Vacuum Assisted Resin Transfer Molding
$n_{N_S}(t_i)$	Experimental observation of nucleation rate for single damages at time t_i
$n_{N_D}(t_i)$	Experimental observation of nucleation rate for double damages at time t_i
$L_S(t)$	Drift of Brownian motion for single damages (i.e. nucleation rate)
$L_D(t)$	Drift of Brownian motion for double damages (i.e. nucleation rate)
a_S	Experimental observation of size of single damages
a_D	Experimental observation of size of double damages

$c_S(t)$ Damage ratio of single damage at time t

$c_D(t)$ Damage ratio of double damage at time t

$\varphi(\mu)$ Rate of change in moisture concentration

D_T Diffusivity of matrix

ACKNOWLEDGMENTS

Firstly, I am thankful to almighty whose guidance and help was always with me to complete this work. I am expressing my deep gratitude and indebtedness to my adviser Dr. Anwarul Haque, the chairman of the thesis committee for his continuous assistance, encouragement and advice during this research. I would also like to appreciate Dr. Zhijian Wu, Department of Mathematics, the University of Alabama for his great involvement and cooperation in the mathematical modeling of this work. I'm also thanking Dr. M. E. Barkey and Dr. S. Roy for being in my committee.

I would like to express my thanks to the MINT center, the University of Alabama where I used the facilities for optical microscopy. My special thanks to Ms. S. A. Chawla for assisting me in manufacturing the composite panels.

I am also thankful to my parents and sister for consistence encouragement from thousand miles. This thesis is a gift for them.

Finally, I am really grateful to the department of Aerospace Engineering and Mechanics, the University of Alabama for supporting my research.

CONTENTS

LIST OF TABLES

LIST OF FIGURES

CHAPTER 1

INTRODUCTION

Composite materials, especially polymer matrix composite (PMC) materials are being used in various aerospace and structural applications due to light weight, high specific strength and stiffness. These PMC based structures are subjected to variable mechanical loading under various environmental parameters such as; temperature, moisture, UV radiation etc. So, it is a matter of concern how the PMC structure will respond during its design life under the effect of these environmental parameters. Several factors such as manufacturing process, mechanical and environmental loading condition, percentage of initial damage/void content etc. influence the durability of the PMC structure. However, the overall strength or stiffness degradation is mostly dependent on damage/microcrack evolution. Presence of damages at the beginning leads to damage evolution in a different manner (such as damage growth rate) compared to the damage evolution from a virgin condition. Moreover, the damage evolution process in PMC is not necessarily a deterministic process especially when environmental parameters come into the scenario. The major environmental parameters such as moisture, temperature, and UV radiation play an interesting role in damage evolution process. Moisture and temperature get diffused into the PMC which leads to breakage or reconstruction of polymer chains because of change in entropy of the molecules. Similarly, UV radiation also affects the structure of the polymer chain. As an overall effect of this phenomenon mico-damage nucleation as well as annihilation occurs. Moreover, the density of damages at any time affect further damage density evolution as well as action of environmental parameters on the PMC. The entire

complicated damage evolution process leads to stiffness or strength degradation of the PMC. In order to predict durability of composites, it is quite important to predict this nature of degradation based on damage density evolution. Hence, in this work the main emphasis is given on proposing a mathematical model for predicting damage densities of the PMC at different time intervals.

The damage density evolution process in PMC under environmental loading is being investigated by the researchers for last few years. However, most of them proposed the damage density as a deterministic parameter for a specific environmental condition. But the case is not same when multiple environmental parameters are involved. This becomes more complicated to determine the exact form of damage density in such situations. Reynolds and McManus (1999) and Roy et al. (2001) studied the damage density evolution in graphite/epoxy composite material under cyclic hygrothermal condition and they represented the experimental observation statistically, rather than deterministically. According to their analysis, the damage density within any time range varies within a certain standard deviation and interestingly this variance also changes with respect to time. However, in order to notice the actual damage density distribution function a rigorous experimental data has to be gathered for a certain condition and this is very time consuming. All of these observations demand for a non-deterministic and simple mathematical model for damage density evolution which is capable to predict damage density from a small number of experimental observations.

In this work, a modified form Liouville's equation (Huang (1987)) is applied as a damage density evolution model. Usually, Liouville's equation is applied in order to predict evolution of probability density function where independent variables of the density function are phase variables. Damage densities can be thought of as analogous to the probability

density of damages which may also be called as “number density of damages”. This terminology is used in developing the mathematical model. Higher/lower damage density at any certain region refers to higher/lower probability of damages or microcracks per unit length or area or volume. Once the environmental parameters are involved, this damage density (we can call damage probability) function no longer remains stationary. As a result the overall or net growth rate in damage density leads to be balanced by term which consists of deviation between damage nucleation rate and annihilation rate. Hence, the uncertainty in damage density evolution process comes from uncertainty in nucleation/annihilation process In this work annihilation rate was observed to be trivial with respect to nucleation rate in affecting damage density evolution process. However, this simplest case is quite meaningful because the difference between nucleation and annihilation rates is net growth rate of damage density and this can be replaced by overall damage nucleation rate i.e. how fast the damages are growing after generation of some more damages as well as healing of some existing damages. As we do not have any prior information about the damage density in a specimen, the Monte Carlo simulation technique is not very effective in this case. “Brownian motion” is used to define the randomness in nucleation rate, they are defined in terms of There is a valid reason behind this which is discussed in chapter 3. The application of this concept leads to generate several nucleation rates based on some limited experimental evidences. So, the solution of the governing damage density evolution equation consists of nucleation rate from experimental observation and standard Brownian motion as an added noise which eventually introduces the damage density as a “Stochastic Process”. The standard Brownian motion does not evolve with respect to time because it is generated from standard normal distribution. The experimental observation (the drift) for certain time interval is used to guide the standard Brownian motion so that it can remain consistently fluctuating within a

variance which will cover the forthcoming damage density in the same environmental condition for a certain specimen. The involvement of added noise to the experimental data benefits us by reducing the number of observations which is very important.

Once the nucleation rate is defined, their involvement in Liouville's equation helps to predict the damage density in two ways. One way is to define the physical parameters of damages such as length; orientation etc. can be correlated with the environmental parameters such as distribution of moisture concentration and temperature inside the material as phase or state variables. All these lead to a generic mathematical model for damage density evolution which can predict damage density at different environmental conditions. However, this requires us to define the "Hamiltonian" of the phase space consisting of the physical and environmental parameters as phase variables which is shown in the generic mathematical model. Configuring this Hamiltonian demands for more thorough experimental analysis of several conditions. Once the Hamiltonian is evaluated, the model can be applied for a certain range of environmental conditions without inspecting crack length, moisture and temperature distribution for any environmental condition within the range. In this case only a limited amount of observations for nucleation rate is necessary. Determining the Hamiltonian needs an in-depth analysis which is not being focused in this work rather the second approach has been followed in order to predict damage density based on the experimental observation. As an alternative way, the modified Liouville's equation can be written as a stochastic ordinary differential equation which consists of only nucleation rate. This form keeps the model limited to predict damage density only for a specific environmental condition. The main emphasis was given on predicting nucleation rate and damage density based on less number of experimental observation even though we may not have the information about damage length, moisture and temperature distribution inside the material. Interestingly, either way is

fine to predict damage density whereas the second method narrows down to a specific environmental condition and this can be considered as a limitation of this method.

The generalized mathematical model is thoroughly discussed in chapter 3. The model is reduced to the simple form based on the fixed environmental condition which is being considered in the experimental validation.

CHAPTER 2

LITERATURE REVIEW

In order to predict the durability of PMC structures several research works have been done in last few years. These works may be classified in four major categories: "Micromechanics model" proposed by Chaim et al. (1989), "Material model" based on time-stress property, proposed by Brinson et al. (1978); Oliveira and Creus (2004), "Structural model" based on analysis of the evolution of the critical elements, proposed by Case and Reifsnider (1996), "Micro-damage model" proposed by Talreja (1985, 1986, 1990 and 1994). The "Material model" considers the viscoelastic behavior of the PMC. The long-term effect on the stress relaxation property (Viscoelasticity) is affected due to the environmental parameters, the stiffness of PMC degrades and this model can predict the long-term stiffness degradation of the virgin PMC from macro-mechanical aspect. "Micromechanics method" starts from the fibers, matrix, and interface; finally relates the prediction based on micromechanics to the macro-mechanical properties. The first three models considered the PMC without any initial micro-voids or defects or in a single word "Damages". But in real life the PMC structures are not totally damage free. Micro-voids arise from the air entrapment during curing and fabrication process. So, it is more reasonable to consider the PMC with initial micro-voids at the starting of its service life as considered by Judd and Wright (1978). Talreja (1985, 1986, 1990, and 1994) predicted the material stiffness reduction due to initial voids or micro-cracks. He introduced a second order damage tensor which is present in the PMC as an initial micro-crack and showed the relationship of the damage tensor with stiffness of the composite material.

Typically the fiber reinforced PMC absorbs moisture in humid environment which further accelerates at high temperature. The initial voids increase the moisture content inside the material. As a result, residual stress is increased which causes micro-crack nucleation. However, these micro-cracks nucleate significantly in matrix and fiber-matrix interface rather than in fiber only. UV radiation and heat conduction cause hardening of the material. This leads to a possibility of developing micro-crack annihilation as well as nucleation. The nucleation/annihilation affects the moisture and temperature diffusion rate inside the PMC (Lundgren et al. (1999)). Combined effect of all these parameters finally causes damage density evolution owing to nucleation and annihilation process. The influence of such nucleation and annihilation of microcracks in composites due to environmental ageing parameters develops microcracks or damages in a distributed fashion rather than a single damage. In general, nucleation and annihilation/coalescence rate of microcracks are eventually linked with damage evolution process in macroscopic level. The damage evolution process is usually influenced by the collective effects of numerous microdamages rather than the singularity of an individual crack as considered in traditional fracture mechanics approach. As a result a statistical theory of microdamage evolution due to hygrothermal ageing parameter is the focus of the present investigation.

The term “damage density” is not always a deterministic parameter particularly in composite materials. It is a very complex parameter that depends on environmental parameters, loading conditions, time as well as nucleation and annihilation rates. In a single sentence, “damage density” is a random time dependent parameter. Reynolds and McManus (1999) observed the crack density evolution under cyclic hygrothermal ageing and they defined this damage density statistically rather than deterministically. The randomness in nucleation and annihilation rate is one of main causes behind random evolution of damage

density which was not discussed in their work. As a consequence, the materials property, such as stiffness is directly influenced by the randomly evolving microcracks or damages. The effect of damage density and moisture absorption on the material stiffness was noticed by Lundgren et al. (1999) in a deterministic manner. In that paper the stiffness change was noticed for a fixed number of damages instead of considering the damage density as random variable. Varna et al. (1999) also showed the evolving crack density on the material stiffness degradation based on experiment. However, they did not come up with any mathematical model for defining crack density from the physical phenomena which can be directly related to the damage tensor. Randomness in damage density evolution process is significantly contributed by the randomness in nucleation/annihilation processes. These two terms are involved in the governing damage density evolution equation (nucleation/annihilation rates). There is no such damage density evolution model available in the literature which considers nucleation and annihilation rates and their randomness in the analysis.

The fundamental concept of the proposed microcrack density evolution model comes from Liouville's equation (See Huang (1963) and Sobczyk (1991), Bai et al. (1991, 1996)). The physical parameters of microcracks such as: length, orientation, geometry etc were considered to be phase variables and the governing equation leads to evaluate number density of damages at a certain combination of phase variables. Besides the deterministic approach, Yu and Youshi (1997) used the similar type of equation for non-deterministic case. However, microcrack or damage number density evolution under environmental degradation was not investigated specifically using the concept of Liouville's equation. In this work Liouville's equation is modified in order to relate the damage density with the overall growth of the damage density or more clearly "nucleation rate". The valid reason behind random damage density evolution is randomness in "nucleation/annihilation rate". There is no straight

forward mathematical model for defining “nucleation/annihilation rate”. It is quite relevant to use experimental observations in order to predict nucleation/annihilation rates. However, in order to define these terms in deterministic form, multiple investigations should be carried out on a large number of samples for establishing a function which can predict these two terms appropriately which is not very practical.

The significant reason behind damage nucleation in PMC matrix is “polymer chain scissioning” and annihilation or healing is occurred due to “polymer chain re-construction”. Both of the processes are conducted to be non-deterministic under certain circumstances. Although the proposed study is not focused at molecular level, the overall outcome of this phenomenon leads to randomness in nucleation/annihilation rates based on experimental observation (Discussed in Chapter 4). Moreover, quantitative analysis of microcrack densities at several time intervals is not totally free of errors. Hence, it is essential to define nucleation rate as stochastic processes due to presence of uncertainties from both of these perspectives. Unfortunately, we do not have any concrete evidence (such as: probability distribution, mean and variance) to configure this uncertainty. In order to mitigate these problems, an alternative approach is required which is invariant of the above parameters. Augusti and Mariano (1999) showed the damage density as a “Sub-semi-martingale” which is quite relevant to the fundamental idea of this work. It is meaningful to say that, damage density evolution in the PMC under environmental loads is random process and the randomness has specific upper and lower bound. In our study the damage density is also shown to be as sub-semi-martingale which depends on the nucleation rate. However, the nucleation rate is defined generically as a semi-martingale (Klebaner (2005)) based on certain valid assumptions (chapter 3) which leads to the damage density as a sub-semi-martingale The main advantage of this definition is to introduce standard Brownian motion

into the nucleation rate. Hence the nucleation rate becomes Brownian motion with drift which is a quite well known form of Brownian motion (Klebaner (2005))). Finally, a simplified mathematical model has been proposed for predicting damage density evolution model that is applicable for any class of damages or microcracks.

CHAPTER 3

MODEL DEVELOPMENT

The physical aspects of the proposed statistical damage evolution model are discussed in this section before presenting the mathematical formulation. It is clearly explained in the work by Bai et al. (1991, 1996) that the mesoscopic damage density in a heterogeneous material (such as composites) may be predicted using Liouville's equation. The length, orientation, spatial position of microcrack tip/centroid, geometry may vary among certain groups of damage. Hence, among all the existing damages, a group of damages can be defined in terms of certain set of physical parameters. At the same time, another class of damage may be defined in terms of different sets of physical parameters. These physical parameters are called as "phase variables" (Papenfuss et al. (2002), Huang (1987) and Sobczyk (1991)) which constructs a unit phase space. Eventually, the phase variables change with time and refer to new groups of microcracks which are being evolved in time. The outcome of these evolving phase variables leads to evolution of probability density of damages in a region of phase space. Li et al. (1996) applied this concept to model microdamage density evolution in glassy polymeric materials without considering the environmental parameters. This invoked the compatibility of Liouville's equation for studying damage evolution due to environmental ageing parameters.

3.1 Generalized Mathematical Formulation

The generalized mathematical model developed in this section is based on Liouville's equation (Bai et al. (1991, 1996), Papenfus et al. (2002)) which is used to deduce a "Forward- Backward Stochastic Differential Equation (FBSDE)". The developed FBSDE

plays an important role in predicting number density of damages using the Brownian motion as nucleation/annihilation rates. This is a new concept incorporated in our proposed model.

3.1.1 Fundamental Concept

The phase variables are classified into two main classes based on the direct or indirect involvement in the damage density evolution (Bai et al. (1991, 1996)):

- Highly sensitive phase variables
- Less sensitive phase variables

We are interested in both cases. The physical parameters such as damage length, orientation, velocity and spatial distribution carry the information for number density of damages under both environmental as well as mechanical loading. Due to environmental parameters such as moisture, temperature, UV radiation cause hygrothermal stress, chemical reaction inside the polymer chain which lead to generation and growth of damages as well as healing of existing damages. It is discussed earlier that environmental ageing parameters such as moisture, temperature, UV radiation and oxidation influences the PMC by different mechanisms like diffusion, conduction, electromagnetic waves etc. Hence, all of the environmental components reside in a local region inside the material, such as:

- Average moisture concentration at any region inside the material
- Average temperature at any region inside the material
- Average hardness at any region inside the material

As mentioned earlier, a group of microdamages can be distinguished from another group by the strong and weak variables. So, we can define the term "Number density of damages" as a quantity which counts the microdamages with length c, orientation ξ, average moisture concentration μ, average hardness h and average temperature T

throughout the region $d\Psi : \langle dt, dx_1, dx_2, dx_3, d\xi, dc, d\mu, dh, d\Phi \rangle$. Hence, we can define number density $n(t, x_1, x_2, x_3, c, \xi, \mu, h, \Phi)$ as:

$$n : [0, t] \times \mathbf{R}_x^3 \times \mathbf{R}_c \times \mathbf{R}_\xi \times \mathbf{R}_\mu \times \mathbf{R}_h \times \mathbf{R}_\Phi \to \mathbf{R}^+ : \mathbf{R} \text{ is real number set} \qquad (1)$$

Here,

x_1, x_2, x_3 : Spatial Coordinates of the damage tip/centroid

c : Damage size

μ : Moisture concentration

h : Hardness at different locations

Φ : Distribution of temperature

$[0, t]$: Time interval

$\mathbf{R}_x^3$: Eucledian space

$\mathbf{R}_c$: Damage length (Any real number)

$\mathbf{R}_\xi$: Damage orientation (Any real number)

$\mathbf{R}_\mu$: Average moisture concentration (Any real number)

$\mathbf{R}_h$: Average hardness (Any real number)

$\mathbf{R}_\Phi$: Average temperature (Any real number)

$\mathbf{R}^+$: Any positive real number

The overall effect of the evolution of number density of damages may be interpreted as net growth in damage density because some new damages are generated and at the same time some existing damages become larger in scale and switches to a different group. In the near time some existing damages may heal too. The overall outcome of this complicated process refers to nucleation as well as annihilation of damages or micro-cracks at a certain state of the phase variables.

3.1.2 Derivation of the Governing Equation

The analogy of the mass or momentum balance equation is applied in the case of number density of damages, i.e. flux of damage flow into and out of the phase space $d\Psi$ is balanced by the difference of nucleation and annihilation of microcracks or damages. Hence, the Liouville's equation can be written in terms of the defined phase variables as (Bai et al. (1991, 1996), Huang (1987), Papenfus et. al. (2002), and Sobczyk (1991)):

$$\frac{dn}{dt} = \frac{\partial n}{\partial t} + \frac{\partial(\mathrm{V}_1 n)}{\partial x_1} + \frac{\partial(\mathrm{V}_2 n)}{\partial x_2} + \frac{\partial(\mathrm{V}_3 n)}{\partial x_3} + \frac{\partial(An)}{\partial c} + \frac{\partial(\Xi n)}{\partial \xi} + \frac{\partial(\varphi n)}{\partial \mu} + \frac{\partial(Hn)}{\partial h} + \frac{\partial(\theta n)}{\partial \Phi} = n_N - n_A \tag{2}$$

The expanded form of the PDE is:

$$\frac{\partial n}{\partial t} + (\overline{\mathrm{V}} \cdot \nabla) n + A\frac{\partial n}{\partial c} + \Xi\frac{\partial n}{\partial \xi} + \varphi\frac{\partial n}{\partial \mu} + H\frac{\partial n}{\partial h} + \theta\frac{\partial n}{\partial \Phi} = f(n, x_1, x_2, x_3, c, \xi, \mu, h, \Phi) + \left(n_N - n_A\right) \tag{3}$$

Where

$n\left(t, x_1, x_2, x_3, c, \xi, \mu, h, \Phi\right)$: Number density of damages

$\mathrm{V}_i = \dot{x}_i$

$A = \dot{c}$

$\Xi = \dot{\xi}$

$\varphi = \dot{\mu}$

$H = \dot{h}$

$\theta = \dot{\Phi}$

$n_N ; n_A$: Damage nucleation and anihillation rates

$$f(n, x_1, x_2, x_3, c, \xi, \mu, h, \Phi) = -n\left(\frac{\partial \mathrm{V}_1}{\partial x_1} + \frac{\partial \mathrm{V}_2}{\partial x_2} + \frac{\partial \mathrm{V}_3}{\partial x_3} + \frac{\partial A}{\partial c} + \frac{\partial \Xi}{\partial \xi} + \frac{\partial \varphi}{\partial \mu} + \frac{\partial H}{\partial h} + \frac{\partial \theta}{\partial \Phi}\right)$$

$\overline{\mathrm{V}} = \mathrm{V}_i \mathbf{e}_i$ ($\mathbf{e}_i$: Unit Vector)

The first term in above equation (3) carries the unsteady behavior of the damage density function "n". The second term refers the damage or micro-crack evolution in terms of spatial locations whereas the 3rd refers to micro-crack growth or dimensional change (crack length) of the micro-crack. The 4th, 5th and 6th terms of the PDE bring environmental degradation in the analysis. On the right hand side, the term $n_N - n_A$ refers to difference between nucleation and annihilation rates; i.e. net nucleation rate of the damage which is the main focus in this work. This term can be simply called as overall growth in number density of damages or how fast the damages are growing inside the material which is in generally a function of $x_i, \xi, c, \mu, h, \Phi$. However, $n_N - n_A$ is defined as a function of time (t) only and annihilation rate is not considered in the experimental validation of the model.

It is discussed earlier that the damage nucleation and annihilation rates in the PMC are not really deterministic under environmental degradation. Lets define them as stochastic processes at any probability state ω: $\{n_{N_t} : t \geq 0\}$ and $\{n_{A_t} : t \geq 0\}$. It is well established that the damage density evolution can be defined as Markov Process (Augusti and Mariano (1999)) and based on this concept it is quite relevant to say, the nucleation and annihilation

rates of damage at a current time influence the nucleation and annihilation rate in the next time step i.e. nucleation/annihilation processes are memory less processes. Hence we can assume that the conditional mathematical expectation "E" of the nucleation or annihilation rates (may be thought as an average of nucleation/annihilation rates for damages at any certain instant can be written in terms of the nucleation/annihilation rate at the previous instant. Referring from Klebaner (2005), we can assume: n_{N_t}, n_{A_t} adapted to the filtration: $\mathbf{F} = \{F_t\}$ on the interval $0 \le s < t \le T$ as (sub-martingale or super-martingale):

$$\begin{aligned} &E\left(\left|n_{N_t}\right|\right) < \infty \qquad \text{or} \qquad E\left(\left|n_{N_t}\right|\right) < \infty \\ &E\left(n_{N_t}\middle|F_s\right) \le n_{N_s} \qquad E\left(n_{N_t}\middle|F_s\right) \ge n_{N_s} \end{aligned} \tag{4.(a)}$$

Similarly, for damage annihilation;

$$\begin{aligned} &E\left(\left|n_{A_t}\right|\right) < \infty \qquad \text{or} \qquad E\left(\left|n_{A_t}\right|\right) < \infty \\ &E\left(n_{A_t}\middle|F_s\right) \le n_{A_s} \qquad E\left(n_{A_t}\middle|F_s\right) \ge n_{A_s} \end{aligned} \tag{4.(b)}$$

From this assumption we can call the damage nucleation and annihilation rates as "*super-martingales*" or "*sub-martingales*". The damage density is defined as "*sub-semi-martingales*" by Augusti and Mariano (1999) because damage density evolution is a random process with bounded variations. Hence it is quite relevant to define the damage nucleation/annihilation rates as subset of "*semi-martingales*" by relaxing the assumption of

bounded variation for these two parameters. Later on we can show the damage number density which is built up based on the nucleation and annihilation rates (semi-martingales) is sub-semi-martingale (Augusti and Mariano (1999)). These two parameters are stochastic processes and hence we can redefine the governing equation for damage evolution for any probability state ω as:

$$\frac{\partial n_t}{\partial t}+(\overline{\nabla}\cdot\nabla)n_t+A\frac{\partial n_t}{\partial c}+\Xi\frac{\partial n}{\partial \xi}+\varphi\frac{\partial n_t}{\partial \mu}+H\frac{\partial n_t}{\partial h}+\theta\frac{\partial n_t}{\partial \Phi}= f(n_t,x_1,x_2,x_3,c,\xi,\mu,h,\Phi)+n_{N_t}-n_{A_t} \tag{5}$$

Now it has become quite important to emphasize on the nucleation and annihilation rates based on our assumption which is still purely mathematical. For predicting number density of damages, these terms has to be defined in such a manner that they do not violate the assumption and at same time they can lead to a solution of equation (5) which is convenient for numerical study of damage number density. Hence the nucleation and annihilation rates can be decomposed in terms of a predictable process and local martingale; Klebaner (2005). The local martingale can consist of standard Brownian motions. So we may write:

$$\begin{aligned} n_{N_t} &= L_1(t)+\beta_1\cdot B_t \\ n_{A_t} &= L_2(t)+\beta_2\cdot B_t \end{aligned} \tag{6}$$

Here, $L_1(t), L_2(t)$ are the predictable processes (in other words drifts of the standard Brownian motion) which may come from prior information (such as experiments) which is

discussed in experimental validation of this model. On the other side, β_1, β_2 refer the weights of the standard Brownian motions B_t (can be called as the volatility of the Brownian motion) by which it gets involved with the predictable process. However, the use of this weight factors leads the Brownian motion to be local martingale because the weight factors depend on locally stopped Brownian motion. In order to construct the Brownian motion, it can be defined in terms of a continuous time Random Walk:

$$B_t \approx \frac{q_{K_{[rt]}}}{\sqrt{r}} + (rt - [rt])\frac{X_{[rt]+1}}{\sqrt{r}} \quad t \geq 0;\ K:\ \text{N-Nucleation,A-Anihillation}$$

$$q_{K_{[rt]}} = q_{K_0} + \sum_{r=1}^{[rt]} X_{[rt]} \tag{7}$$

Where

$X_{[rt]}$: Random numbers generated from standard normal distribution

$E(X_{[rt]}) = 0$ and $Var(X_{[rt]}) = 1$

$q_{N_o} = 0; q_{A_0} = 0$ Initial nucleation and anihillation rates

$[rt]$: Integer part of $"rt"$

r : Sample size

It is known that Brownian motion is the limiting case of Random Walk model (Sidney (1992)); so it is quite relevant to define the Brownian motions in terms of continuous Random walk model. We can define the nucleation/annihilation rates in terms of random walk as:

$$n_{N_t} = L_1(t) + \beta_1 \cdot \left(\frac{q_{N_{[rt]}}}{\sqrt{r}} + (rt - [rt]) \frac{X_{[rt]+1}}{\sqrt{r}} \right)$$
$$n_{A_t} = L_2(t) + \beta_2 \cdot \left(\frac{q_{A_{[rt]}}}{\sqrt{r}} + (rt - [rt]) \frac{X_{[rt]+1}}{\sqrt{r}} \right) \quad (8)$$

Before getting into the solution of Equation (5) we need to elaborate the advantage of using Brownian motion in equations (6) and (8). In addition to being continuous time martingales, standard Brownian motion has a significant property: $Var(B_t) = t$. This nature of Brownian motion is very important from the perspective of estimating catastrophe in the structure. This feature may help us to generate the terms n_{N_t}, n_{A_t} in such a manner that the level of uncertainty is increased with respect to time, i.e. if we have a limited number of experimental observations for limited time $t \in T^*, T^* < T$ and the uncertainty keeps increasing as the prediction goes beyond the available experimental data for $t > T^*$ So, Brownian motion with drift (See Equations (6) and (8)) leads to predict the local variations or fluctuations around $L_1(t)$ or $L_2(t)$ which allows us to have less number of experimental data rather than having a large number of observations. This is very important from the perspective of economic damage inspection in structures. However, Brownian motions are almost surely continuous random functions of time at any probability state (Øaksendal (2002)). Sometimes it has sudden jump discontinuity which is also very important feature too. By using Brownian motion, it is possible to analyze the situations when either nucleation or annihilation rates have sudden instabilities/jumps due to any change in loading or environmental condition.

Using the initial condition of number density of damages, the damage evolution equation (Equation (5)) at any probability state ω:

$$\frac{\partial n_t}{\partial t}+(\bar{\nabla}\cdot\nabla)n_t+A\frac{\partial n_t}{\partial c}+\Xi\frac{\partial n_t}{\partial \xi}+\varphi\frac{\partial n_t}{\partial \mu}+H\frac{\partial n_t}{\partial h}+\theta\frac{\partial n_t}{\partial \Phi}=f(n_t,x_1,x_2,x_3,c,\xi,\mu,h,\Phi)+n_{N_t}-n_{A_t}$$
$$n_{t_0}=g(t_0) \tag{9}$$

The above differential equation contains Brownian motions on the right hand side. Apparently, the left hand side of the above equation has to be differentiable where as on the right hand side the Brownian motion is continuous but non-differentiable. Hence, in order to get rid of this inconsistency the equation (9) can be converted to standard form of Ito's "Forward Stochastic Differential Equation (FSDE)" with initial condition ($n_{t_0}=g(t_0)$) (Øaksendal (2002), Jin and Yong (2007)) as (Appendix):

$$dn_t=f(n_t,t,x_i,c,\xi,\mu,h,\Phi)dt+L(t)dt+\beta B_t dt \tag{10}$$
$$n_{t_0}=g(t_0)$$

The function $f(n_t,t,x_i,c,\xi,\mu,h,\Phi)$ consists of time as well as other phase variables. However, the stochastic differential equation is based on time and hence the notation for number density is used as n_t. Here, for simplicity we have written the above equation such as:

$$L(t) = L_1(t) - L_2(t) \tag{11}$$

$$\beta B_t = \left(\beta_1 - \beta_2\right) B_t$$

This FSDE (equation (10)) can be solved for any $t \in [0,T]$ using Ito's formulation (Øaksendal (2002),) which can be written as:

$$n_t = g(t_0) + \int_0^t f(n_t, t, x_i, c, \xi, \mu, h, \Phi)dt + \int_0^t L(t)dt + \int_0^t \beta B_t dt \tag{12}$$

More generally, we can write the solution in terms of integral of standard Brownian motion (most common form):

$$n_t = g(t_0) + \int_0^t f(n_t, t, x_i, c, \mu, h, \Phi)dt + \int_0^t L(t)dt + \beta\left(tB_t - \int_0^t tdB_t\right) \tag{13}$$

Based on the solution of the FSDE, we can extend this formulation to more sophisticated version which contains a "Backward Stochastic Differential Equation (BSDE)". The purpose of including BSDE is to keep the final solution attenuated by both FSDE and BSDE. The generalized form of this BSDE with terminal condition ($\overline{n_T} = \gamma(n_T)$) in the interval $[0,T]$ can be written as:

$$-d\overline{n_t} = F(t, n_t, \overline{n_t}, \underline{n_t})dt + G(t, n_t, \overline{n_t}, \underline{n_t})dB_t \qquad (14)$$

$$\overline{n_T} = \gamma(n_T)$$

There are some interesting issues we can notice from the above equation, such as: the above BSDE is also concerned about number density of damage $\overline{n_t}$ which is different from the solution from FSDE. This stochastic differential equation is constructed based on n_t which is obtained from forward equation (equation (13)) and a predictable process $\underline{n_t}$ (preferably experimental observation of number density of damage). The functions $F(t, n_t, \overline{n_t}, \underline{n_t})$ and $G(t, n_t, \overline{n_t}, \underline{n_t})$ have to be formed in such a manner that can have ability to attenuate the final solution for damage number density using the predicted number density from FSDE as well as experimental observation. It is clearly seen in equations (13-14), the FSDE requires initial condition $g(t_0)$ and BSDE requires terminal condition $h(n_t(T))$ (Jin and Yong (2007))). One can imagine the difference between these two equations: FSDE forecasts the number density of damages based on some known initial information whereas the BSDE uses the final predicted result from FSDE and attempts to trace the number density of damage in a reverse order of time. The generalized model for predicting number density of damage evolution consists of both FSDE and BSDE. Hence, the equations (13-14) are applied together which is called "Forward-Backward Stochastic Differential Equation (FBSDE)" in a combined form. The solution of the BSDE in the interval $[t,T]$ is associated with the solution from FSDE can be written as:

$$\overline{n_t} = \gamma(n_T) - \int_t^T F(t, n_t, \overline{n_t}, \underline{n}_t)dt - \int_t^T G(t, n_t, \overline{n_t}, \underline{n}_t)dB_t \qquad (15)$$

The three versions of number density of damage have different significance. Equation (9) is converted to FSDE in order to form the coupled FBSDE. As it is seen in equation (13), the solution from FSDE (n_t) consists of higher level of uncertainty in long term prediction than the solution from BSDE ($\overline{n_t}$). However, if we look at the limits of integrals in equations (12) and (15) it is clearly seen that interval $[0,T]$ is split into two subintervals: $[0,t]$ and $[t,T]$. As a result FSDE and BSDE (consists of $\underline{n}_t$ from the experiment) can be applied on first and second subintervals respectively. Hence, the overall solution for number density of damages can be written in terms of the triplet $\left(n_t, \overline{n_t}, \underline{n}_t\right)$ or the weighted average of these three solutions:

$$N_t = \frac{W_1 n_t + W_2 \overline{n_t} + W_3 \underline{n}_t}{3} \qquad (16)$$

Here, W_1, W_2, W_3 are the corresponding weights which are involved in the final solution based on the combined effectiveness of the solutions from FSDE n_t, BSDE $\overline{n_t}$ and the adaptive process $\underline{n}_t$.

3.2 Simplification of the Generalized Model

The developed mathematical model for predicting number density of damages is in a generic form. We must define the phase variables corresponding to a certain condition. It is

important to notice that the involvement of different phase variables dependent on the individual environmental condition. If the environment is entirely dry it may not be appropriate to incorporate moisture concentration as a phase variable whereas for hygrothermal loading condition both moisture and temperature can be considered. If hygrothermal load is coupled with mechanical load the phase variables should be defined in a different manner than that of purely hygrothermal loading condition. It is recommended to form the FBSDE based on the experimental observation of an individual environmental condition.

In our case the phase variables considered are: damage length (c) and moisture concentration (μ). Only the nucleation rate are considered. The initial condition for FSDE (n_{t_0}) is determined from the experiment (discussed in Chapter # 4). Based on the analysis of experimental observation, the BSDE is formed. The idea is to use the BSDE in order to attenuate the prediction from forward equation. In this regard, the backward equation is to be formed in such a manner which can deduct the deviation ($|n_t - \underline{n}_t|$) from known terminal condition ($\overline{n_T}$) by reducing random fluctuation ($\sigma n_t dB_t$) coupled with predicted number density of damages from FSDE (n_t) by weight factor σ. It is to be noted that, the terminal condition is based on first few experimental data within the time interval $\left[0, T^*\right]$. However, the proposed FBSDE is being used to predict further number density of damage in the interval $\left[T^*, T\right]$. So, the FBSDE has to be defined on the overall time interval $\left[0, T\right]$ which contains the sub-intervals: $\left[0, T^*\right]$ and $\left[T^*, T\right]$. The terminal condition at $t = T$ is assumed to be same as at $t = T^*$. This leads to the following FBSDE:

$$dn_t = f(n_t, t, c, \mu)dt + atdt + \beta B_t dt \tag{17}$$

FSDE

$$n_{t_0} = \underline{n}_{t_0}$$

$$-d\overline{n_t} = \sqrt{\left|n_t - \underline{n}_t\right|}dt + \sigma dB_t \tag{18}$$

BSDE

$$\overline{n_T} = \underline{n}_{T^*} \approx \underline{n}_T$$

The initial condition and terminal condition are kept in deterministic form. The nucleation rate is written in the form: $(at)dt + \beta B_t dt$; in this expression the term $L(t)$ is considered as a best fitted linear function of time generated from a limited number of experimental observations for nucleation rate. Besides the nucleation rate, number density of damages from experimental observation $\underline{n}_t$ is defined as a best fitted linear function of time within the interval $\left[0, T^* \middle| T^* < T\right]$. The arbitrary constants of the best fitted straight lines are determined from the available experimental data which is discussed in later chapters. Hence, the analytical solutions for the both equations can be written as:

$$n_t = \underline{n}_{t_0} + \int_0^t f(n_t, t, c, \mu)dt + \int_0^t atdt + \beta\left(tB_t - \int_0^t tdB_t\right) \tag{19}$$

$$\overline{n_t} = \underline{n}_T - \int_t^T \sqrt{\left|n_t - \underline{n}_t\right|}dt - \sigma\int_t^T dB_t \tag{20}$$

The term $\underline{n}_t$ is obtained from the experimental observation on the interval $\left[0, T^*\right]$, this can be written as:

$$\underline{n}_t = d_1 + d_2 t : \tag{21}$$

d_1, d_2 are constant for this best fitted linear function of time

Hence, equation (16) can be applied to evaluate the overall number density of damages.

3.3 Numerical Scheme for Solving the FBSDE

The solution of simplified form of the FBSDE (equation (19 and 20)) is still in purely mathematical form. The Brownian motions are to be represented in the form of random walk model (equations (7-8)) and Euler-Maruyama (EM) method (Iacus (2008)) is applied in order to solve the FSDE (equations (17-18)). The discrete version of the solution of FBSDE can be written as:

For any $j : 1 - l_e$ (22)

$$n_{t_j} = n_{t_{j-1}} + f(n_{t_{j-1}}, t_{j-1}, c_{j-1}, \mu_{j-1})\Delta t + \left[a_1 + a_2 t_{j-1}\right]\Delta t + \beta B_{t_{j-1}}\Delta t$$

$$n_{t_0} = \underline{n}_{t_0}$$

$$\overline{n_{t_j}} = \underline{n}_T - \sum_{k=j}^{l_e} \sqrt{\left| n_{t_k} - \underline{n}_{t_k} \right|} \Delta t_k - \sigma \sum_{k=l_e-j}^{l_e} \left(B_{t_k} - B_{t_{k-1}} \right) \tag{23}$$

$\underline{n}_T$: Terminal value obtained from experiment

$T = l_e \Delta t$; l_e is an integer

$$B_{t_j} = \left[\frac{q_{N_{\lfloor rt_j \rfloor}}}{\sqrt{r}} + (rt_j - [rt_j]) \frac{X_{\lfloor rt_j \rfloor + 1}}{\sqrt{r}} \right]$$

$$q_{N_{\lfloor rt_{j-1} \rfloor}} = q_{N_0} + \sum_{r=1}^{\lfloor rt_{j-1} \rfloor} X_{\lfloor rt_{j-1} \rfloor}$$

The above equations are used in validation of proposed model based on experimental observation. Once the solutions are obtained from equations (22 and 23), the weighted average number density of damage (N_t) is evaluated from equation (16).

CHAPTER 4

QUANTITATIVE ANALYSIS OF DAMAGES AND MOISTURE CONCENTRATION FROM EXPERIMENTAL OBSERVATION

The model described in chapter 3 has been verified experimentally using accelerated environmentally aged specimens. In the following sections a brief description of laminate fabrication process, specimen preparation, ageing experiments, damage inspection and quantitative analysis of damages are outlined.

4.1 Manufacturing and Sample Preparation

The vacuum assisted resin transfer molding (VARTM) process was used to manufacture graphite/epoxy composites with orientation $\left[0/90^0/90^0/90^0\right]_S$. The reinforcing carbon fiber (Magnamite Unsized Fiber, Hexel Corporation) was impregnated by SC-15 epoxy resin manufactured by Polymeric Inc. An experimental setup of VARTM process is shown in Fig:1. In this process resin was impregnated over stacked graphite fiber through distribution mesh under vacuum pressure. A resin pot was used in between the exit port and the vacuum pump to trap excess resin. The resin impregnated panel was cured at room temperature for 48 hours. A number of samples with dimension ($1\,\text{inch}\times 1\,\text{inch}\times 0.1\,\text{inch}$) were cut from the cured panel for environmental ageing experiments. The specimens were polished at the edge before placing in environmental chamber for damage inspection.

Figure 1. Experimental setup for manufacturing composite panel

4.2 Environmental Ageing and Damage Inspection

The images were snapped by the image acquisition system attached to the optical microscope for quantitative damage analysis. The initial state of damages was observed for each specimen and later they were put under ageing cycle as shown in Figure 2. The specimens were kept in water at 65^0C -70^0C for approximately twelve weeks in three weeks segments (segment-1, segment-2 and segment-3 in Figure-2) and then they were placed in dry condition at room temperature for four weeks after each segment. This leads to hygrothermal cycling which promotes damage evolution process.

4.3 Damage Inspection Scheme

The quantitative analysis of damages was recorded based on the total time interval which is represented in terms of normalized time. Hence, the quantitative analysis of damages and the mathematical model for damage prediction is based on entire time history of the damage density instead of any localized time interval.

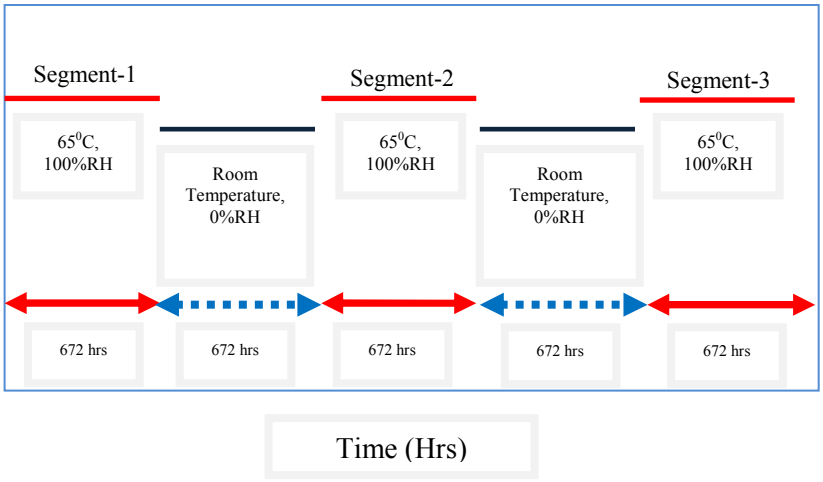

Figure 2. Applied environmental condition at different time intervals

The objective is to introduce a repetitive fluctuation in hygrothermal strain which causes hygrothermal fatigue and eventually damages are introduced in the specimens. This hygrothermal cycling is most common in real life case instead of a monotonous environmental condition.

At different stages of ageing period, the specimens were taken for damage inspection and they were put back to the oven once the inspection is over. The damages were inspected from polished edge of each specimen under optical microscope (model: Lietz) with 20x magnification at different times of ageing. At every inspection a number of images were collected at different locations (around the similar location where initial observation was done) on the edge of specimen for further quantitative analysis. The magnification of $20\times$ is convenient to capture damages within the scale of $10^{-3}-10^{-4}$ square inch which covers a large range in the scale of damages. However, it is important to classify the damages of different scales in order to predict number density of damages within a certain scale. The number density evolution of large damages are more likely to be deterministic than

comparatively smaller damages. Once the damages are classified, the proposed model for number density of damage evolution in chapter 3 can be applied to damages of a certain scale (class). Before getting into the detail analysis, it is necessary to preprocess the stored images in order to arrest damages of different scales which are discussed in the next sub-section.

4.3.1 Preprocessing of Captured Images

It is to be noted that all the captured images possess same area. This was done by setting the same aperture and magnification (20x) in the CCD camera. Each image was divided into 48 (six rows and eight columns) sub-regions of area $1.25\mu\text{m}^2\left(\approx 0.04\text{inch}^2\right)$ which was observed to be appropriate for arresting or capturing damages of different scales.

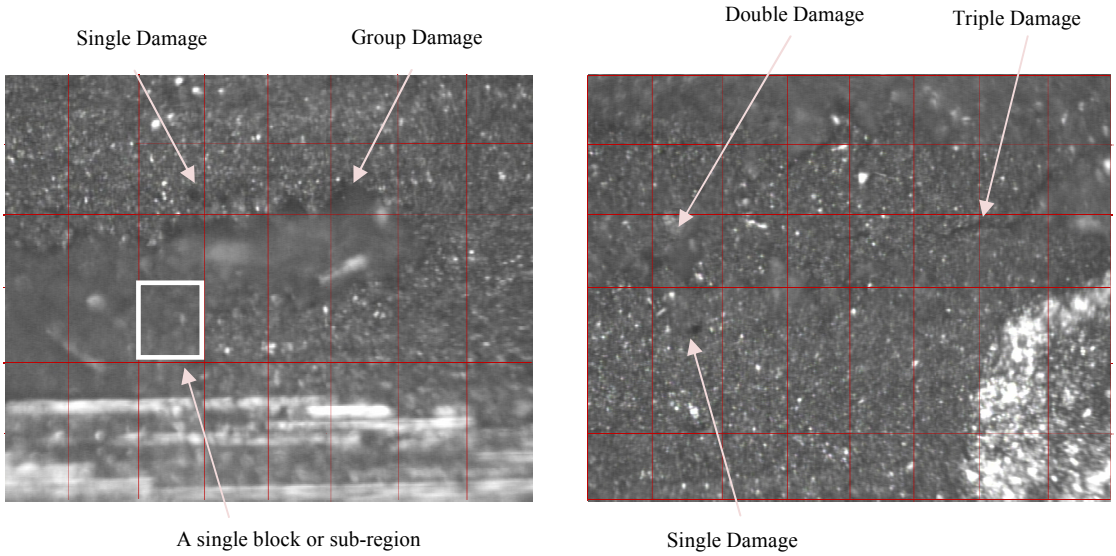

Figure 3. Damages of different scales captured in the equal area sub-regions

4.3.2 Damage Classification Scheme

The damages were classified based on the number of "*sub-regions or blocks*" which were occupied by a damage or part of damage. Some of the damages reside entirely in

a single block whereas some cover two or three consecutive blocks. In some cases damages cover a large number of sub-regions. It was observed that some damages were difficult to capture in a single image and these damages usually occupy a large number of blocks. Such damages were more deterministic in nature than the ones which stayed in a single or double blocks. As a result, it is important to classify the damages according to their size. Analogous to the classification scheme proposed by Reynolds (1998), we have identified different types damages based on the number of blocks covered by them in order to quantify the damage density for a certain group of damages from optical microscopic observation as shown in Figure 3. The following nomenclatures were used in identifying different types of damages.

- Single Damage: Damages occupying one sub-region
- Double Damage: Damages occupying or residing in two sub-regions
- Triple Damage: Damages occupying or residing in three sub-regions
- Large Damage: Damages occupying or residing in four sub-regions
- Group Damage: Damages occupying or residing in five or more sub-regions

The present work mostly focused in single and double damages since they were considered to be non-deterministic in nature. It is to be noted that, all classes of damages except single damages are superposition of single damages. As mentioned earlier, a group of single or double damages infers to the number density which evolves with respect to time. This classification scheme leads to evaluate the nucleation rate and number density for damages of any class of interest which has to be collaborated to the model.

4.3.3 Quantitative Analysis of Damages

The damage classification scheme as defined earlier leads to determining the nucleation rate and number density of a certain class of damages from the microscopic examination of aged specimens. These parameters were kept dimensionless.

4.3.3.1 Nucleation Rate

Nucleation rate refers how fast damages are growing with respect to time. This is a critical parameter in the model for predicting number density of damages. The experimental observation for nucleation rate at any arbitrary time t_i depends on the number of damages at previous time interval t_{i-1} . This can be determined using the following equations:

$$n_{N_S}(t_i) = \left(\frac{\begin{array}{r}\text{Number of sub-regions occupied by single damages at time } t_i - \\ \text{Number of sub-regions occupied by single damages at time } t_0\end{array}}{\frac{t_i - t_0}{T}} \right) \quad (24)$$

$$n_{N_D}(t_i) = \left(\frac{\begin{array}{r}\text{Number of sub-regions occupied by double damages at time } t_i - \\ \text{Number of sub-regions occupied by double damages at time } t_0\end{array}}{\frac{t_i - t_0}{T}} \right) \quad (25)$$

Where

$n_{N_S}(t_i)$: Nucleation rate of single damage at time t_i

$n_{N_D}(t_i)$: Nucleation rate of double damage at time t_i

t_0 : Initial time

T : Length of overall time interval

At different times, a typical (not average) trend of nucleation rates for single and double damages can be shown in (Figure 4(a)-4(b)). The standard deviation is shown to represents the variation of nucleation rate:

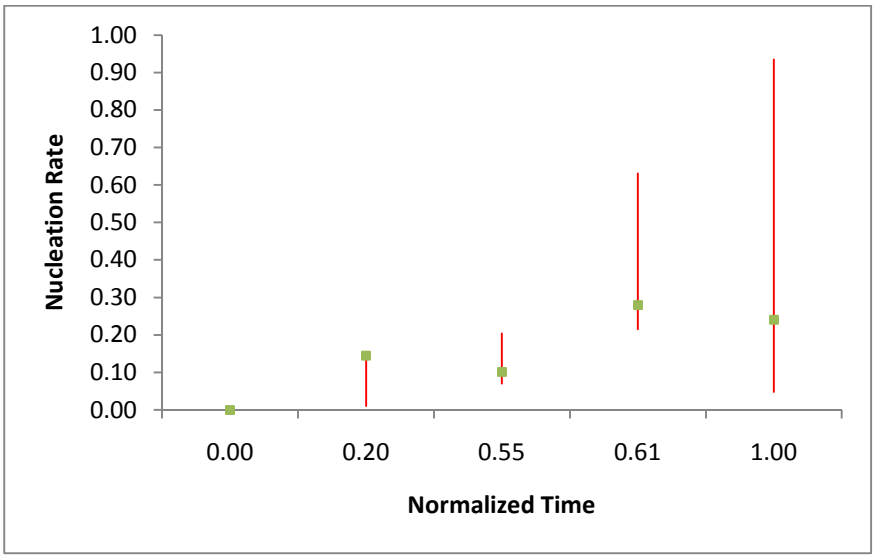

Figure 4(a). Experimental observations for nucleation rate of single damages

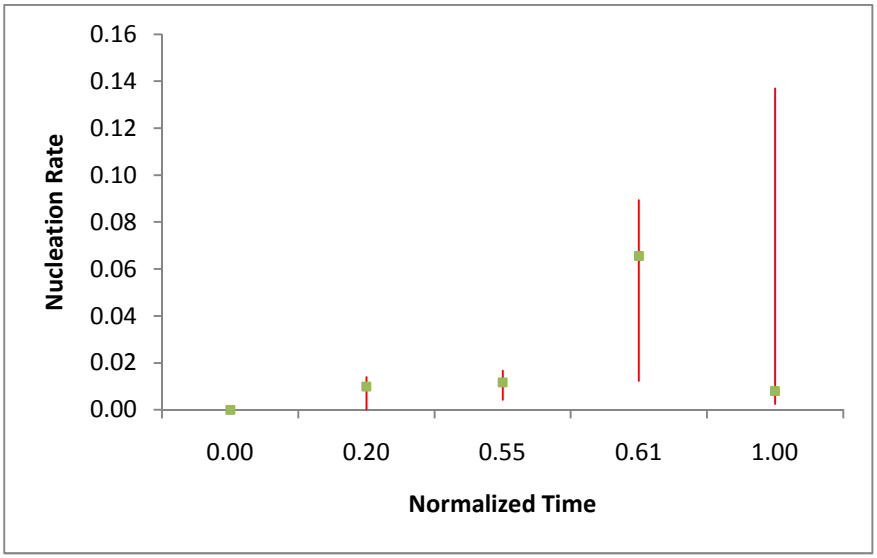

Figure 4(b). Experimental observations for nucleation rate of double damages

In Figures 4(a) and 4(b), the nucleation rates are represented within the overall time interval 672hrs $\times 5$ segments (Figure 2) which is normalized for convenience.

The experimental observations in both Figure 4(a) and 4(b) clearly reveal the randomness in nucleation rate as time increases. The nucleation rate is observed to be more consistent at earlier stage. As time increases the variance is also seen to be increased. This intensifies the evidence for introducing Brownian motion in order to model nucleation rates as $Var(B_t) \propto t$. In order to mitigate this problem, nucleation rate is defined as a Brownian motion with drift (equation 6) and this drift ($L_1(t)$) is extracted implementing the first three experimental observations which is used with the standard Brownian motion. Later on the nucleation rate containing Brownian motion was used to predict further data points. This has been discussed in next chapter. Based on the first few data, the drift for single and double damages (Figure 4(a) and 4(b)) may be defined as follows:

Table-1: Average drifts for Brownian motions based on first three experimental observations

Single Damage	Double Damage
$L_S(t) = 0.2738t$	$L_D(t) = 0.024t$

4.3.3.2 Number Density of Damages

The number density of damages of any class is understood as probability of microscopically damaged region. In general it is the chance of having damages of a certain class within a certain time interval or probability of blocks which are occupied by a specific class damages (based on the terminology mentioned in subsection 4.3.2) within a time interval. So, the formulae to evaluate the number density at any time t_i are:

$$N_S(t_i) = \frac{\text{Total number of sub-regions occupied by single damages at time } t_i}{\left(\text{Total number of images considered at time } t_i\right) \times 48} \tag{26}$$

$$N_D(t_i) = \frac{\text{Total number of sub-regions occupied by double damages at time } t_i}{\left(\text{Total number of images considered at time } t_i\right) \times 24} \tag{27}$$

The experimental observation for number density of single and double damages is shown below:

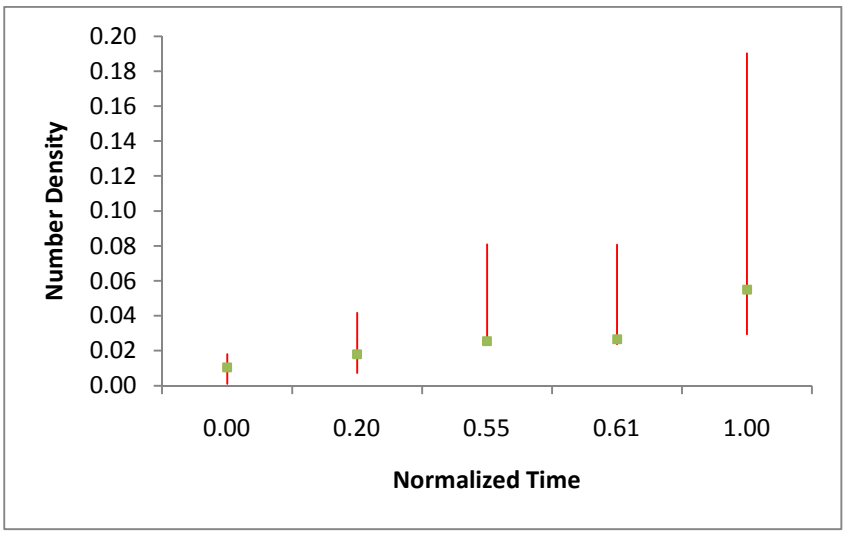

Figure 5(a). Experimental observations for number density of single damage

Similar to nucleation rates, first four experimental observations for number density of damages may be represented as best fitted first order polynomials. The first order polynomial is incorporated in the Backward Stochastic Differential Equation (equation (20) and (21)), ($\underline{n}_t$). Table-2 shows all the best fitted first order polynomials with the corresponding coefficients d_1, d_2 for $\underline{n}_t$ (Equation (21)).

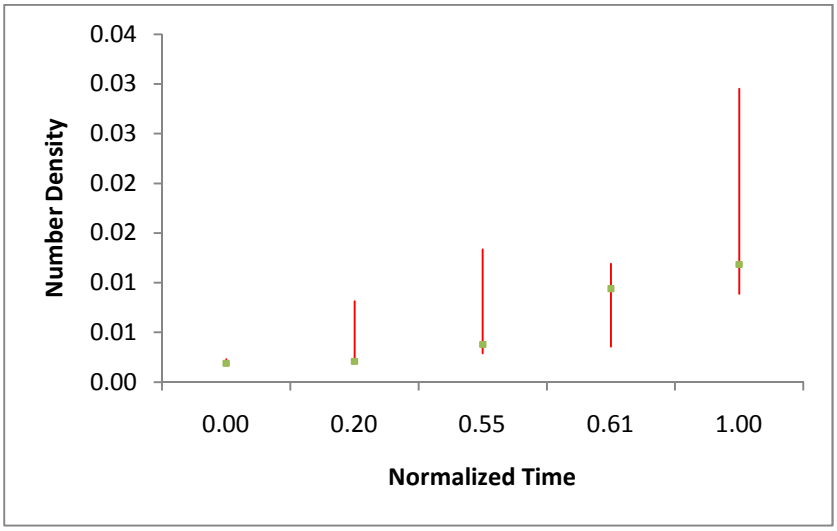

Figure 5(b). Experimental observations for number density of double damage

Table-2: Representation for typical number density of damages from first three experimental observations

Single Damage	Double Damage
$\underline{n}_{t_S} = 78.9\times10^{-3}t + 5.27\times10^{-3}$	$\underline{n}_{t_D} = 10.4\times10^{-3}t + 2.57\times10^{-3}$

4.3.3.3 Damage Growth

It is important to observe the size of damages in a specific class and their average growth with respect to time. As an example, the class "single damage" represents a group of damages which entirely reside in a block. However, damages of a certain class do not imply all the damages are of same size (length, area or volume).

Damages of a certain class (in our case single or double) refer to a group of damages of size (area) lying in the range: $a_{S_{\max}} \le a_S \le a_0$ or $a_{D_{\max}} \le a_D < 4a_0$, a_0 is the area of smallest

damage existing in the specimen at initial stage. The quantity a_0 is approximated to $\frac{a_{S_{\max}}}{16}$ ($\approx 78.12\mu m^2$) as evident from Figure 6:

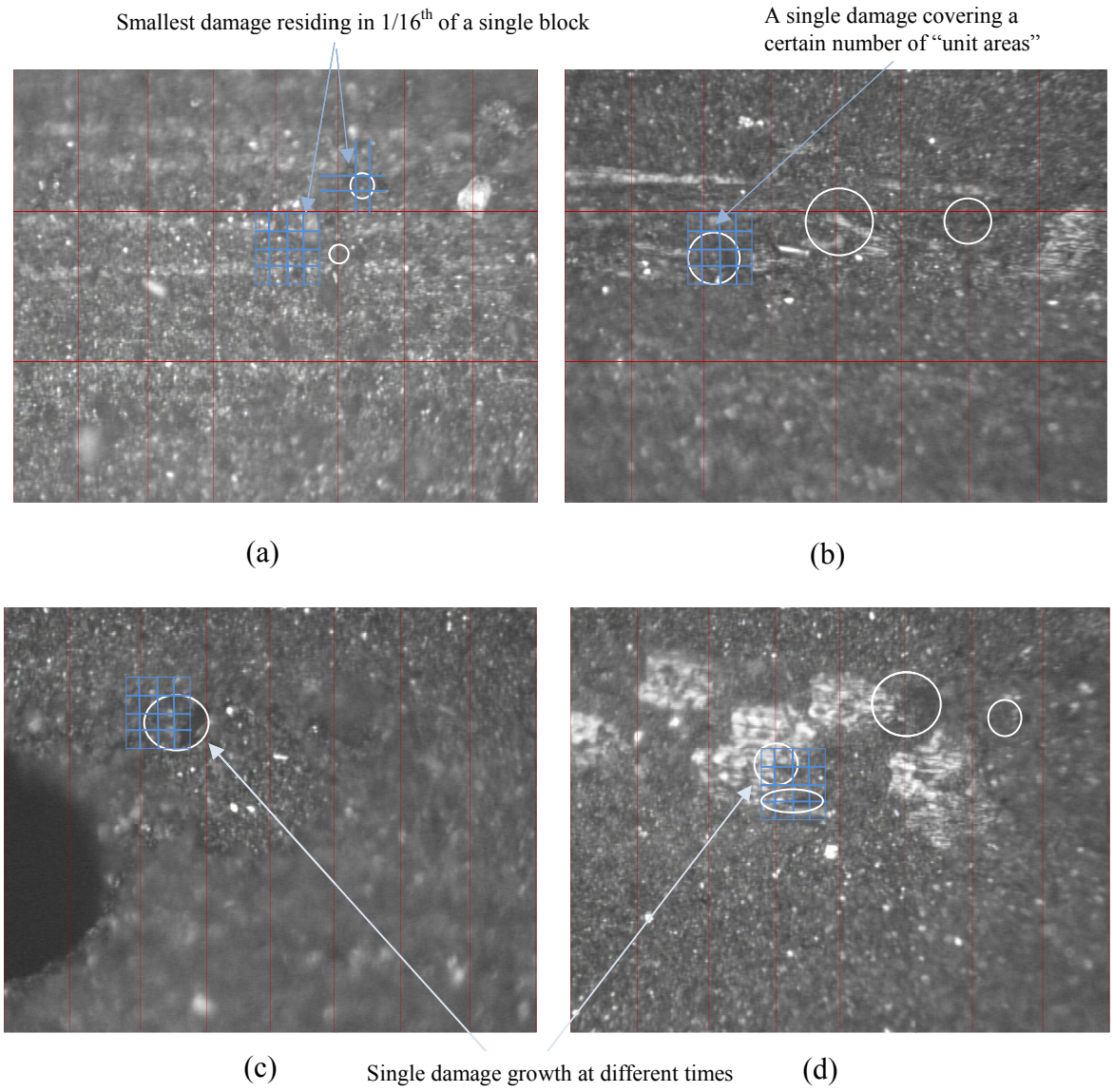

Figure 6. Damage growth in a specific specimen at different times

Here, a_S and a_D are any arbitrary areas of single or double damage, respectively. Based on observation (Figure 6(a)), each block can be divided into 4×4 equal sub-blocks of area approximately equal to area of smallest damage (a_0). We can call a_0 as "unit area of

damage" and hence, we can define the area of single or double damages as multiple of a_0 (functions of time). Mathematically, the more meaningful expression to define damage growth can be represented in terms of ratio between a_S (or a_D) and a_0. This is analogues to "damage ratio" which is defined as "c" in equation (2):

$$\text{Single Damage Ratio} \qquad c_S(t) = \frac{a_S(t)}{a_{S_{\max}}} \tag{28}$$

$$\text{Double Damage Ratio} \qquad c_D(t) = \frac{a_D(t)}{a_{D_{\max}}} \tag{29}$$

Hence, the ranges can be defined as: $\frac{a_S(t)}{a_{S_{\max}}} \le c_S(t) \le 1$ and $\frac{a_D(t)}{a_{D_{\max}}} \le c_D(t) < 1$; for single and double crack, respectively. Using the above two equations, we can calculate the damage growth rate which are supposed to be related to "damage ratio". Before getting into detail discussion of damage growth rate, the average damage ratios for single ($c_S(t)$) and double ($c_D(t)$) damages obtained from experimental observation can be shown as:

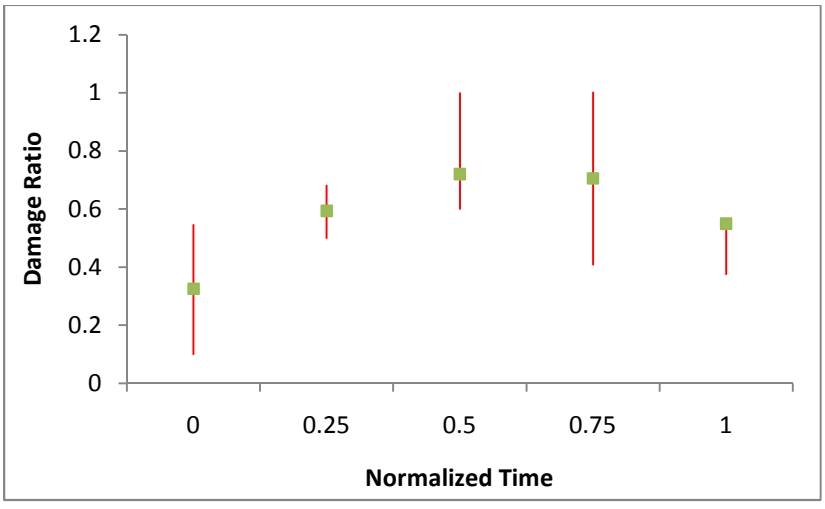

Figure 7(a). Experimental observations for growth of single damages

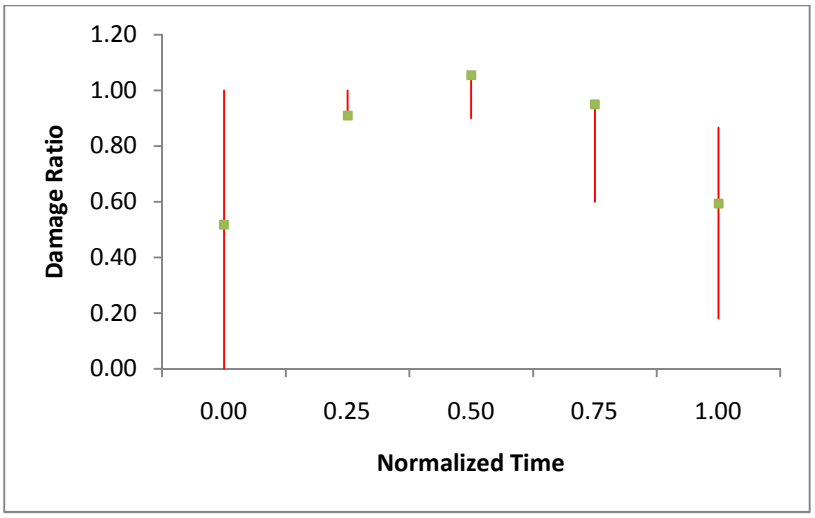

Figure 7(b). Experimental observation for growth of double damage

Once the damage ratio is calculated (Figure 7(a) and 7(b)), we can calculate damage growth rate $\frac{\partial A}{\partial c}$ at any instant t by using the chain rule (equation (3)):

$$\begin{aligned} \frac{\partial A_S}{\partial c_S} &= \left(\frac{\partial A_S}{\partial t}\right) \Big/ \left(\frac{\partial c_S}{\partial t}\right) \\ \frac{\partial A_D}{\partial c_D} &= \left(\frac{\partial A_D}{\partial t}\right) \Big/ \left(\frac{\partial c_D}{\partial t}\right) \end{aligned} \tag{30}$$

Here, we can define $c(t)$ based on experimental observation and hence, $A(t) = \dot{c}(t)$.

4.3.4 Moisture Concentration

In the previous subsections a thorough quantitative analysis is carried out in order to extract most suitable information of damages such as nucleation rates, number density of damages and damage growth rates. There parameters are directly related to damage evolution

process. As we know from earlier discussion that the effect of environmental parameters on the material is influenced by the status of damages in the material. In this work we considered a cyclic hygrothermal loading at three different stages (Segment-1, Segment-2 and Segment-3) followed by room temperature condition. The hygrothermal load causes moisture diffusion inside the specimens. Due to progressive evolution in number density of damages, the moisture diffusion process is influenced and hence diffusion coefficient is not fixed at different stages of ageing. The variation in diffusion of moisture leads to variation in average moisture concentration through the thickness of the specimen which is defined as a phase variable in the evolution equation (equation (2)). Before getting into the detail discussion on "average moisture concentration", it is important to observe the variation in moisture diffusivity at different stages (segment-1, segment-2 and segment-3) of aging. The diffusivity can be calculated from the following formula (Collings and Stone (1985)):

$$D = \pi \left(\frac{h}{4M_\infty} \right)^2 \left(\frac{M_2 - M_1}{\sqrt{t_2} - \sqrt{t_1}} \right)^2 \tag{31}$$

h: Laminate thickness (0.06inch $\approx$ 1.524mm)

M_∞: Moisture equilibrium level for a given humidity (3.07% for SC-15 at $70^0 C$)

M_i: % of moisture uptake at any time t_i

$\frac{M_2 - M_1}{\sqrt{t_2} - \sqrt{t_1}}$: Slope of the linear portion of the moisture uptake data

Hence, the average diffusivity (D) in segment-1, segmen-2 and segment-3 can be obtained as:

Table-3: Average Moisture Diffusivity in different segments (with standard deviation)

Segment-1	Segment-2	Segment-3
2.08×10^{-4} in^2 / s $\pm1.57\times10^{-4}$ in^2 / s	9.63×10^{-6} in^2 / s $\pm1.59\times10^{-6}$ in^2 / s	1.44×10^{-5} in^2 / s $\pm2.25\times10^{-6}$ in^2 / s

Our primary goal is to calculate average moisture concentration throughout the thickness of the specimen. This moisture concentration is considered to be a phase variable which is involved in the damage number density evolution equation. It is interesting to observe the moisture concentration at different stages of aging (segment-1, segment-2 and segment-3) which is related to number density of damages. In order to calculate average moisture concentration the following equation is used which is proposed by Lundgren et al. (1999)):

$$\mu = \mu_0 + \left(M - \mu_0\right)\sum_{m=1}^{\infty}\frac{8}{\nu_m^2}e^{-\nu_m^2\tau};\tau \geq 0 \tag{32}$$

The fiber volume fraction is calculated at the beginning of the experimental observation which is within the range: $60\%-70\%$. The average moisture concentration is kept as a non-dimensional term and independent of spatial coordinates. The typical "average moisture concentration" calculated from above equation is shown as:

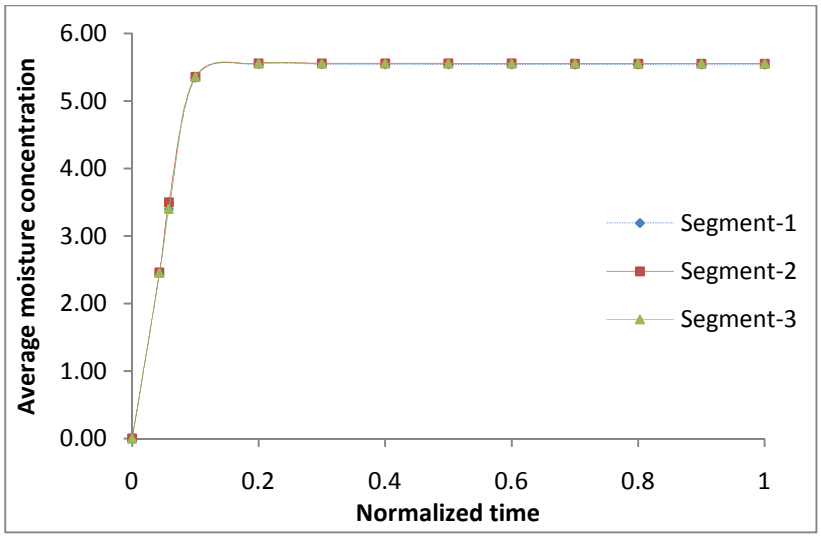

Figure 8. Average moisture concentration in three different segments

The average moisture concentration changing rate with respect to average moisture concentration is similar for all the specimens shown in Figure 8. However, a thorough analysis is required in order to reach a conclusion which is not emphasized in this work. As we have three different segments of ageing at three different time intervals but equal sub-intervals on the overall aging period $T = 5 \times 672$ hrs (Figure 2), the term $\varphi(\mu)$ can be represented in a compact form:

$$\varphi(t) = \frac{\partial \mu}{\partial t} = \frac{\partial \mu}{\partial \tau}\frac{\partial \tau}{\partial t} = \frac{-(M_\infty - \mu_0) D_T \sum_{m=1}^{\infty} 8 e^{-\nu_m^2 \tau}}{L^2} \tag{33}$$

Hence, the derivative of $\varphi(\mu)$, $\frac{\partial \varphi}{\partial \mu}$ can be written in terms of t as (equation (3)):

$$\frac{\partial \varphi}{\partial \mu} = \frac{\frac{\partial \varphi}{\partial t}}{\frac{\partial \mu}{\partial t}} = \frac{\sum_{m=1}^{\infty} \nu_m^2 e^{-\nu_m^2 \frac{D_T t}{L^2}}}{\sum_{m=1}^{\infty} e^{-\nu_m^2 \frac{D_T t}{L^2}}} \tag{34}$$

Here,

Initial moisture concentration $\mu_0 = 0$

Moisture equilibrium level $\mu_I = 3.07$ (which is M_∞)

$$\tau = \frac{D_T t}{L^2}$$

$$D_T = D\left(1 - 2\sqrt{\frac{\text{Fiber Volume Fraction}}{\pi}}\right)$$

$$\nu_m = (2m-1)\pi$$

m : Number of iterations

CHAPTER 5

MODEL VERIFICATION

In this chapter the experimental observations of damage parameters are compared with the same predicted from the proposed stochastic damage evolution model. The experimental observations of damages developed during time interval T^* are incorporated into the FBSDE mentioned in eqns. 22 and 23. This leads to a prediction in number density of damages from the numerical simulation of the FBSDE. The predicted result obtained from the FBSDE is compared with experimental observation for the extended time interval $T_e : \left[T^*, T \right]$.

In this study both single damage and double damage were analyzed thoroughly based on the parameters listed in Table 4. It is to be noted that these parameters are solely related to the construction of Brownian motion and its involvement in the FBSDE eqns.22 and 23:

Table 4: List of parameters which affect the predictability of the proposed FBSDE

- Total number of increments:l_e
- Incremental size:Δt
- Sample size:r
- Volitility of Brownian Motion in nucleation rate (FSDE):β
- Volitility of Brownian Motion in BSDE:σ

5.1 Case-I: Single Damages

The average nucleation rate (drift) was obtained from experimental observation throughout segment-1 and segment-2 as shown in Figure 2. The proposed form of nucleation rate $n_{N_{s_t}}$ in Equation (8) can be written as:

$$L_S(t) = 0.2738t$$

$$n_{N_{s_t}} = 0.2738t + \beta \cdot \left(\frac{q_{N_{[rt]}}}{\sqrt{r}} + (rt - [rt]) \frac{X_{[rt]+1}}{\sqrt{r}} \right) \tag{35}$$

It is to be noted that the selection of drift for constructing nucleation rate of single damage is computed from first few experimental observations. A typical form of nucleation rate is defined in equation (35). The drift (see Table 1) term is computed based on first three experimental observations in order to predict further nucleation rates. An appropriate selection of the parameters mentioned in Table-4 for single damages is:

$$\begin{aligned} l_e &= 100 \\ \Delta t &= 0.01 \\ r &= 100 \\ \beta &= 1 \\ \sigma &= 1 \text{ (For BSDE)} \end{aligned} \tag{36}$$

Hence, the predicted nucleation rate for single damages is shown in Figure 9:

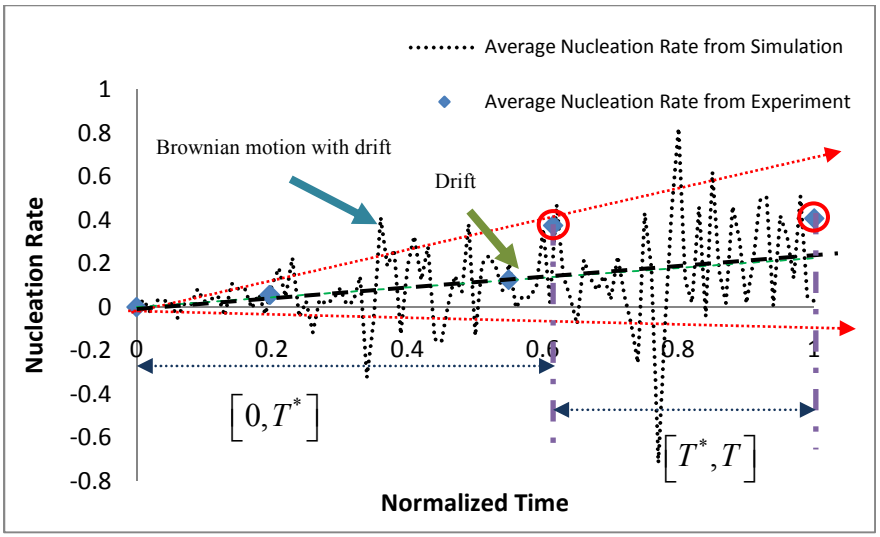

Figure 9. Predicted nucleation rate of single damages by using Brownian motion ($l_e = 100, \Delta t = 0.01, r = 100, \beta = 1$)

In Figure 9, the drift of Standard Brownian motion is defined based on first three observations and the variance (shown in two arrows) generated by using Brownian motion. The Brownian motion with drift in Figure (9) fluctuates within a range (shown with two arrows) which contains last two data points (encircled) of nucleation rate obtained from experimental observation in segment-3.

The predicted nucleation rates for other sets of values for $l_e, \Delta t, r, \beta$ are not seen to be very consistent with the experimental observation as shown in Figures (10-13):

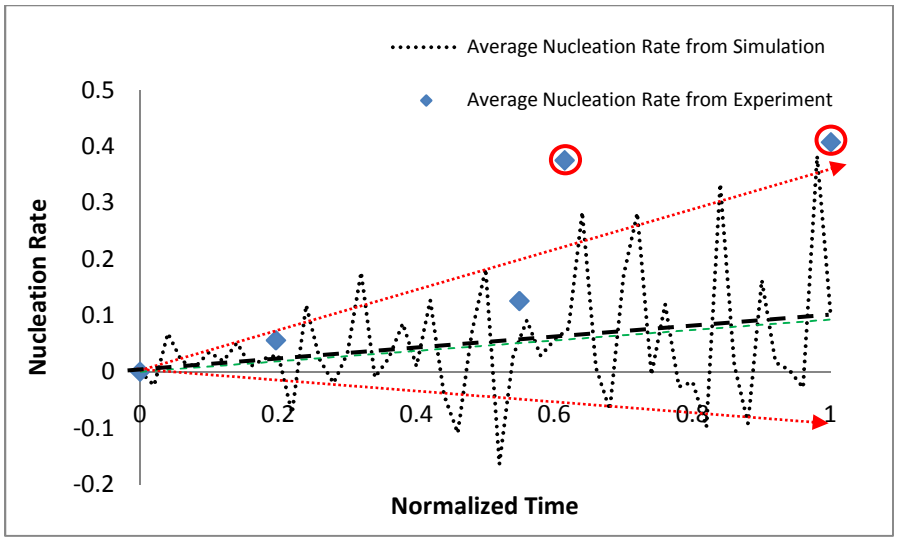

Figure 10. Predicted nucleation rate of single damages by using Brownian motion ($l_e = 50, \Delta t = 0.01, r = 100, \beta = 1$)

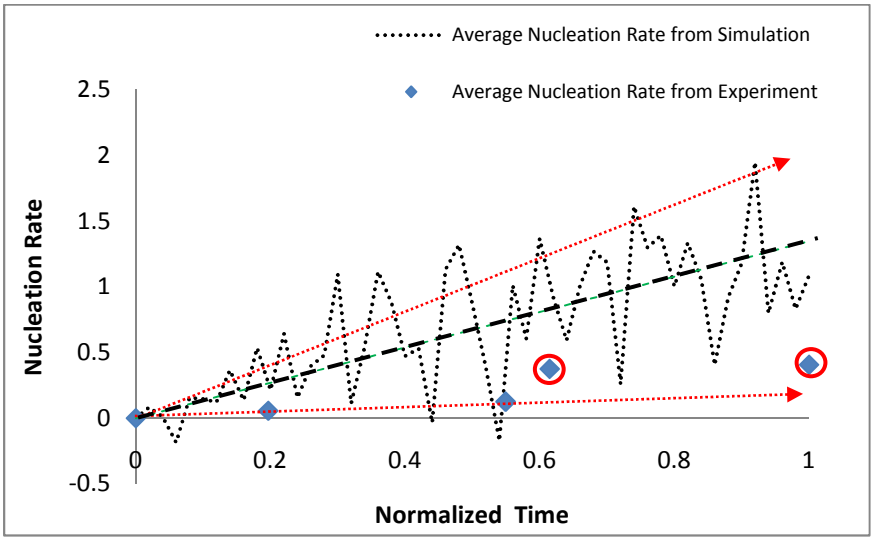

Figure 11. Predicted nucleation rate of single damages by using Brownian motion ($l_e = 50, \Delta t = 0.1, r = 100, \beta = 1$)

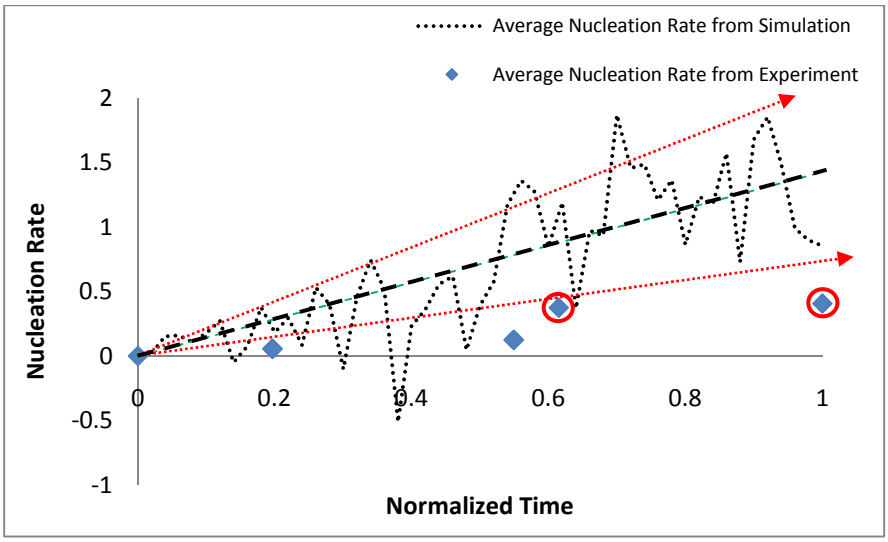

Figure 12. Predicted nucleation rate of single damages by using Brownian motion ($l_e = 50, \Delta t = 0.001, r = 50, \beta = 1$)

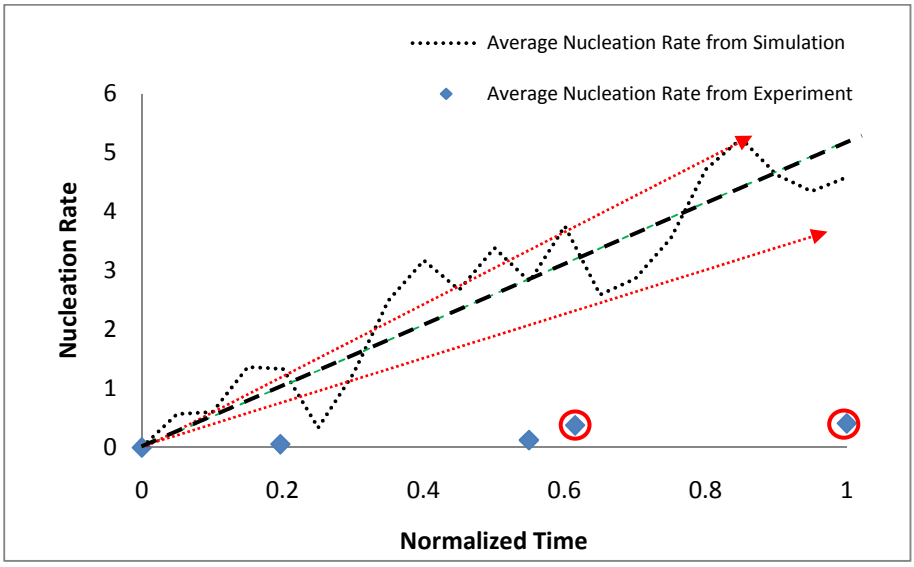

Figure 13. Predicted nucleation rate of single damages by using Brownian motion ($l_e = 20, \Delta t = 1, r = 100, \beta = 1$)

It is to be noted that the predictions shown in Figures 10 - 13 are not consistent with the experimental observation. The prediction in Figure 10 with $l_e = 50$ increments is not as

good as for 100 increments shown in Figure 9. However, for other cases, incremental size is kept either greater or less than $\Delta t = 0.01$ which lead to either over prediction (Figures 11 and 13) or under prediction of nucleation rate (Figure (12)).

Once the nucleation rate is determined, number density of single damages is predicted by using proposed FBSDE (equations 22-23). Finally, average number density of damages (N_{t_S}) is calculated by using equation (16). The term $\underline{n}_t$ in equation (23) is defined based on first three experimental observation of number density of single damages. Hence, this term is defined as: $\underline{n}_{t_S} = 78.9\times10^{-3}t + 5.27\times10^{-3}$ in the FBSDE (Table-2).

For $l_e = 100, \Delta t = 0.01, r = 100, \beta = 1, \sigma = 1$, the predicted number density of single damages from FSDE (n_t), BSDE ($\overline{n_t}$) and average number density of damages from experimental observation ($\underline{n}_{t_S}$) are presented in Figure 14:

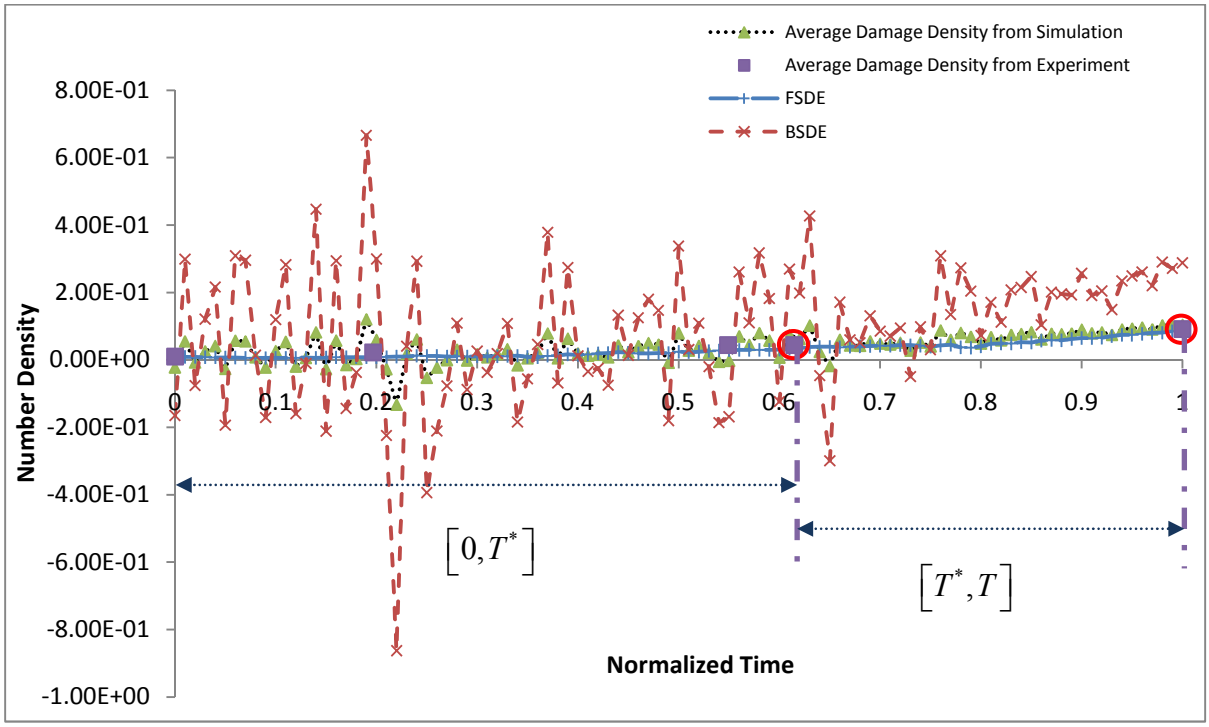

Figure 14. Predicted number density of single damages by using Brownian motion ($l_e = 100, \Delta t = 0.01, r = 100, \beta = 1, \sigma = 1$)

There are few important observations noted in Figure 14. Firstly, the average number density of single damages (N_{t_S}) is quite consistent with the experimental observation. However, the predicted number density of single damages from BSDE is quite erratic but consistent with the experimental observation. The fluctuation is possibly due to non-cumulative nature of BSDE and cumulative nature of FSDE. FSDE keeps coagulating all the uncertainty with respect to time and BSDE keeps splitting the uncertainty in backward direction of time (equations 22-23).

As it is seen in Figures 11-13 predicted nucleation rate is not consistent with the experimental observation for other sets of parameters. Similarly, number density (N_{t_S}) of single damage is also not consistent for the sets of parameters other than $l_e = 100, \Delta t = 0.01, r = 100, \beta = 1, \sigma = 1$ as shown in Figures (15-18):

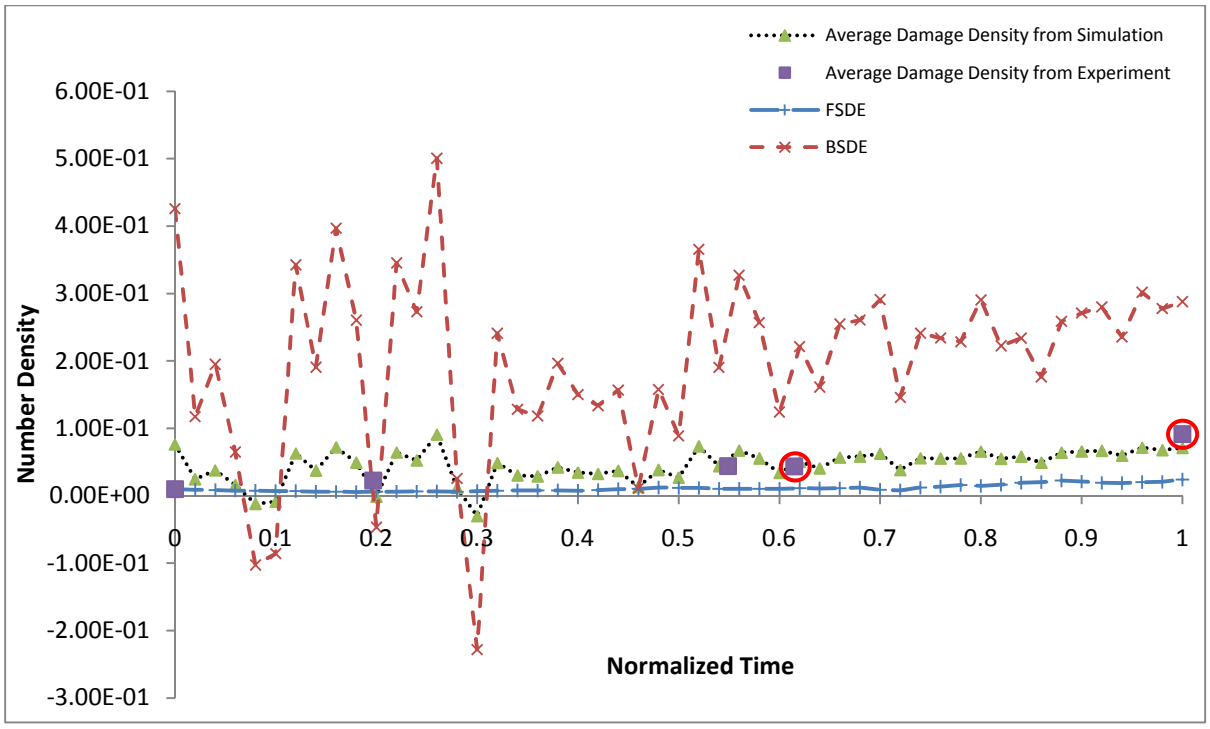

Figure 15. Predicted number density of single damages by using Brownian motion ($l_e = 50, \Delta t = 0.01, r = 100, \beta = 1, \sigma = 1$)

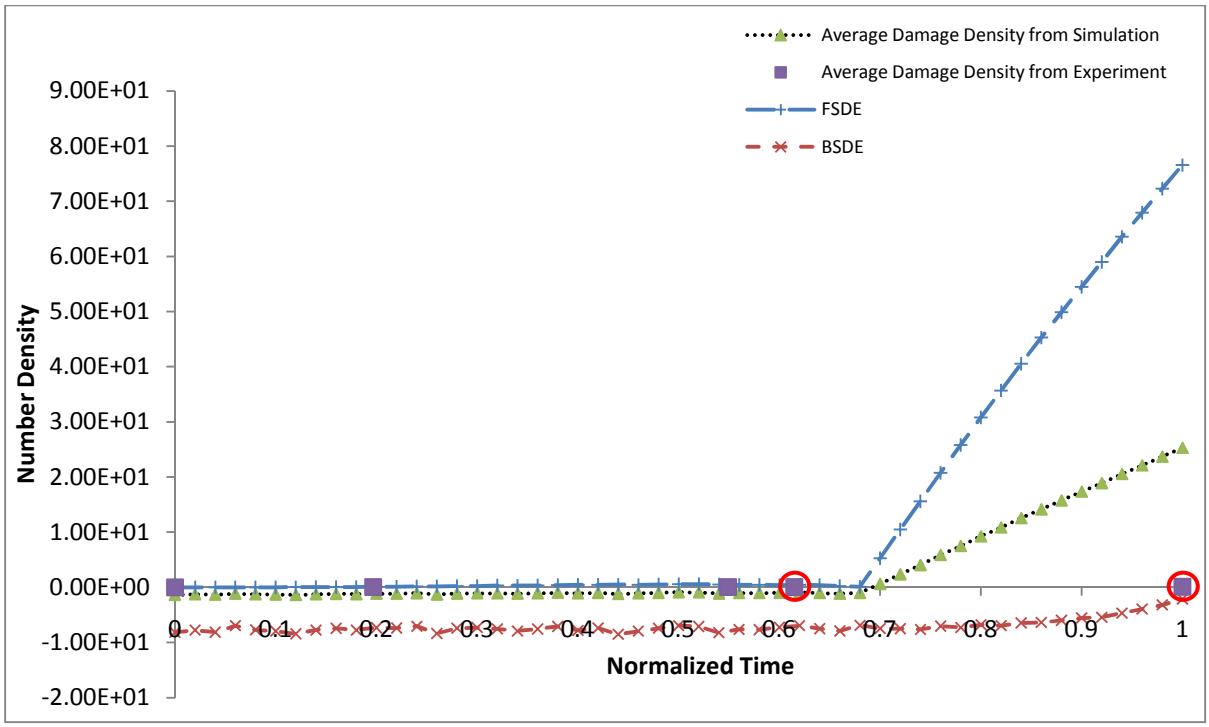

Figure 16. Predicted number density of single damages by using Brownian motion ($l_e = 50, \Delta t = 0.1, r = 100, \beta = 1, \sigma = 1$)

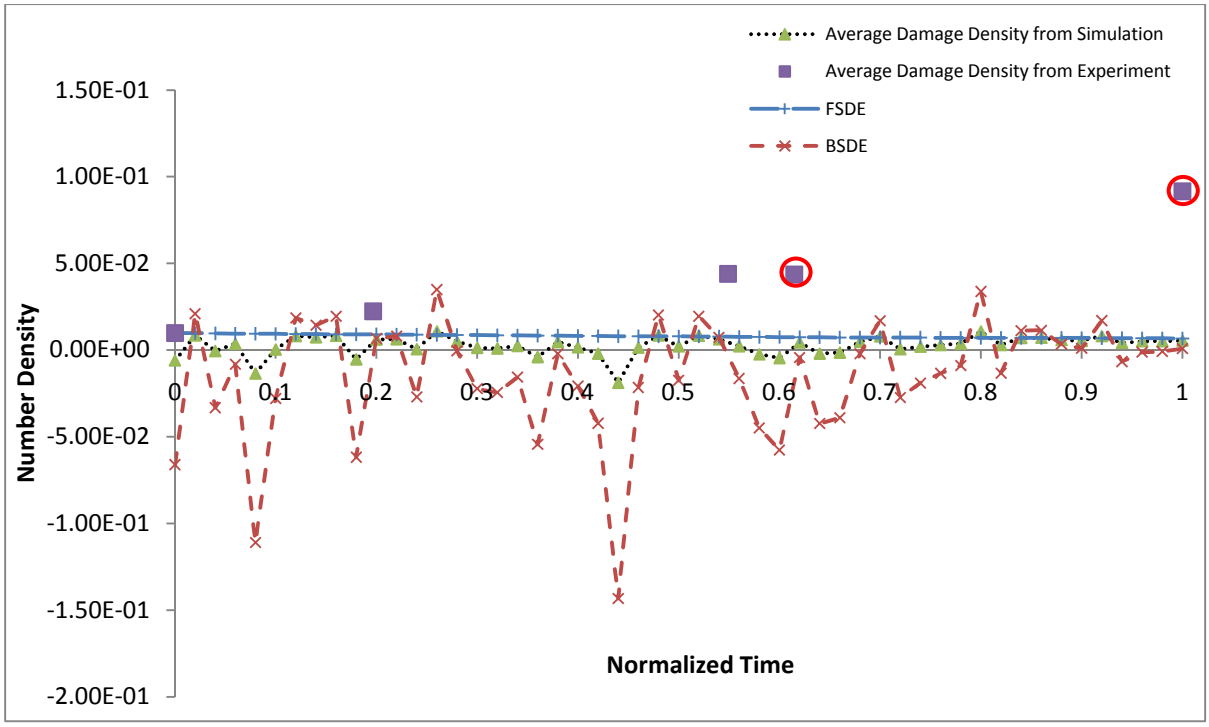

Figure 17. Predicted number density of single damages by using Brownian motion ($l_e = 50, \Delta t = 0.001, r = 50, \beta = 1, \sigma = 1$)

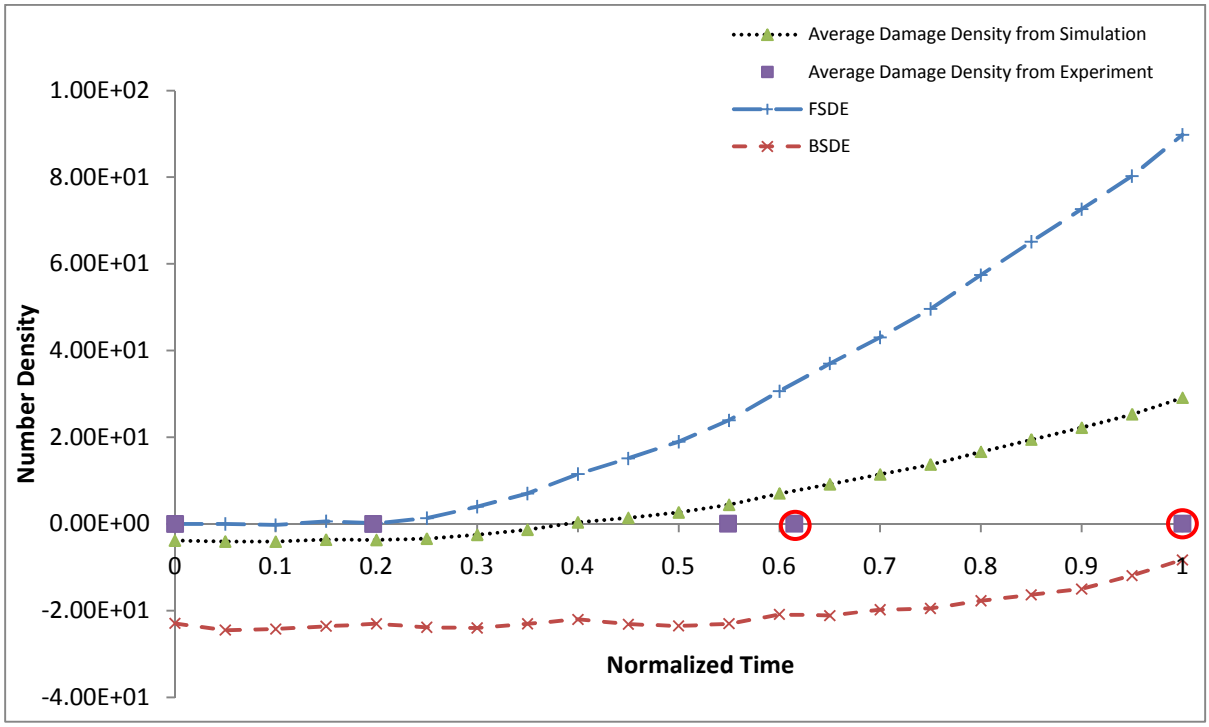

Figure 18. Predicted number density of single damages by using Brownian motion ($l_e = 20, \Delta t = 1, r = 100, \beta = 1, \sigma = 1$)

The predicted number density (N_{t_S}) of single damages is not very consistent even if the total number of iterations becomes half ($l_e = 50$) (Figure 15). However, interestingly prediction from BSDE is better than the FSDE in this case. In other cases Figures 16-18) for different values of l_e are found to be not capable is predicting number density properly. Hence, it is realized that, any appropriate set of parameters is very important to have a meaningful and better prediction.

5.2 Case-II: Double Damages

Similar to single damages, the proposed FBSDE is used to predict nucleation rate as well as number density of double damages. It is obvious to expect the nucleation rate and number density of double damages to be less than single damages. Based on the consistency with experimental observation a set of parameters are to be defined which is listed as follows:

$$\begin{aligned} l_e &= 100 \\ \Delta t &= 0.002 \\ r &= 100 \\ \beta &= 1 \\ \sigma &= 1 \end{aligned} \tag{37}$$

Recalling from Table-1, we can write the nucleation rate for double damages:

$$\begin{aligned} L_D(t) &= 0.024t \\ n_{N_D t} &= 0.024t + \beta \cdot \left(\frac{q_{N_{[rt]}}}{\sqrt{r}} + (rt - [rt]) \frac{X_{[rt]+1}}{\sqrt{r}} \right) \end{aligned} \tag{38}$$

The smaller drift $L_D(t) = 0.024t$ (based on first three experimental observations) for constructing nucleation rate of double damages leads to selection of smaller incremental size because of the fractal behavior of Brownian motion. Based on the above set of parameters the nucleation rate is shown in Figure 19:

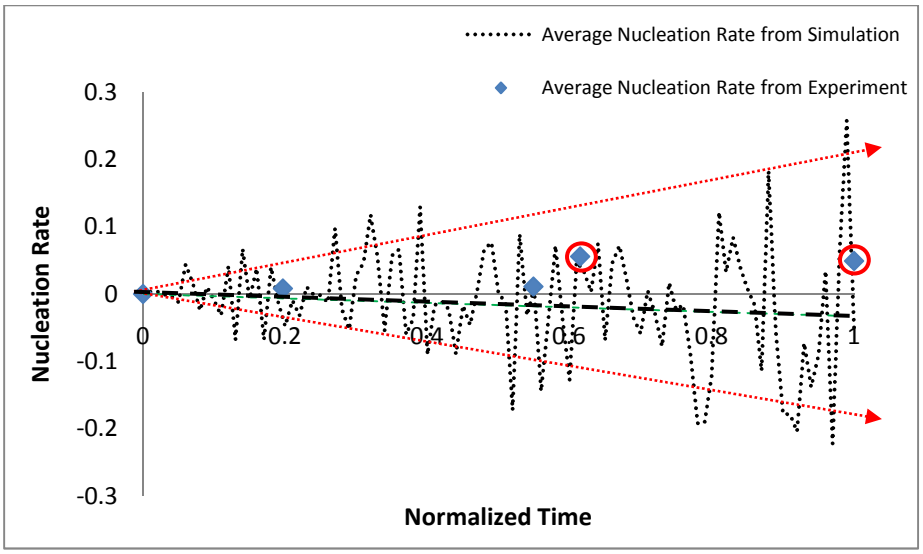

Figure 19. Predicted nucleation rate of double damages by using Brownian motion ($l_e = 100, \Delta t = 0.002, r = 100, \beta = 1$)

In above figures, the variance of the predicted nucleation rate is able to estimate last two experimental observations. However, different sets of parameters were implemented to predict nucleation rate which are shown in Figures 20-22:

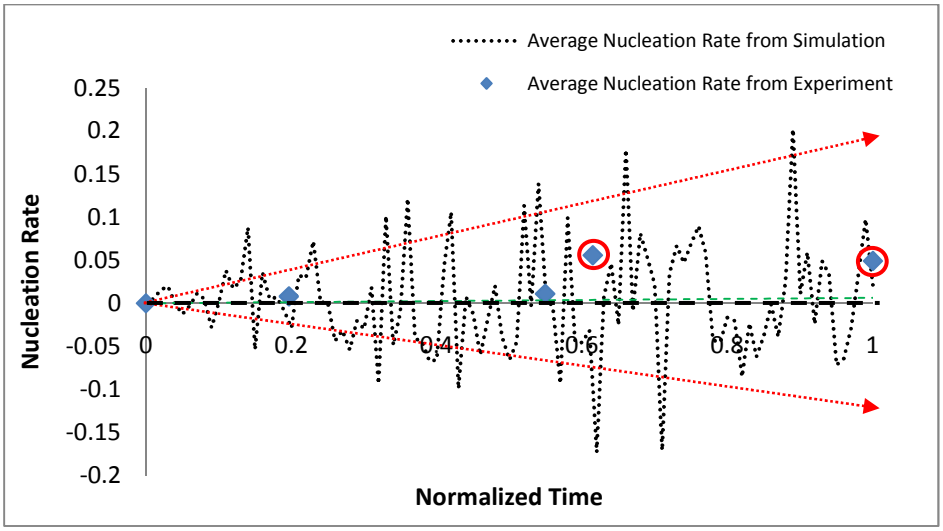

Figure 20. Predicted nucleation rate of double damages by using Brownian motion ($l_e = 100, \Delta t = 0.0015, r = 100, \beta = 1$)

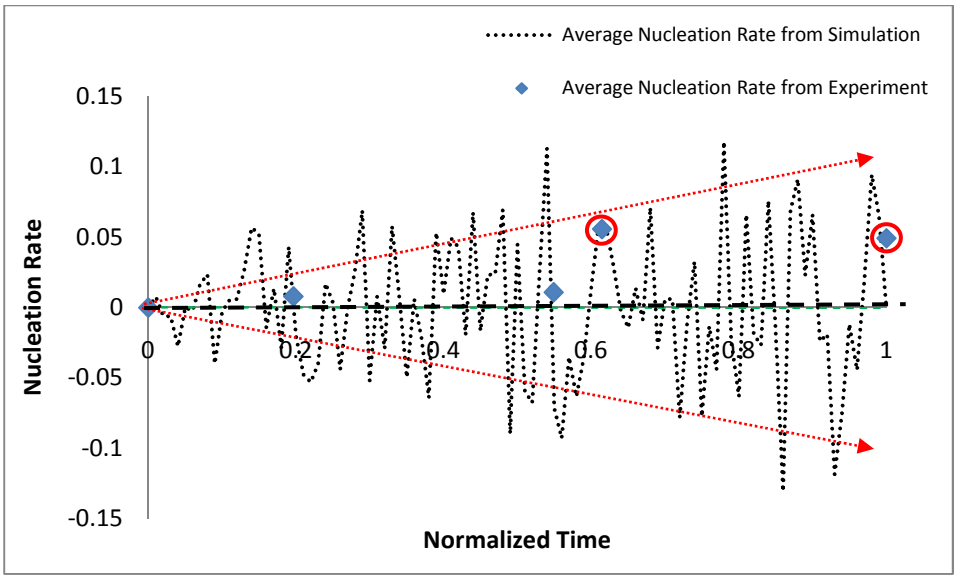

Figure 21. Predicted nucleation rate of double damages by using Brownian motion ($l_e = 100, \Delta t = 0.01, r = 100, \beta = 1$)

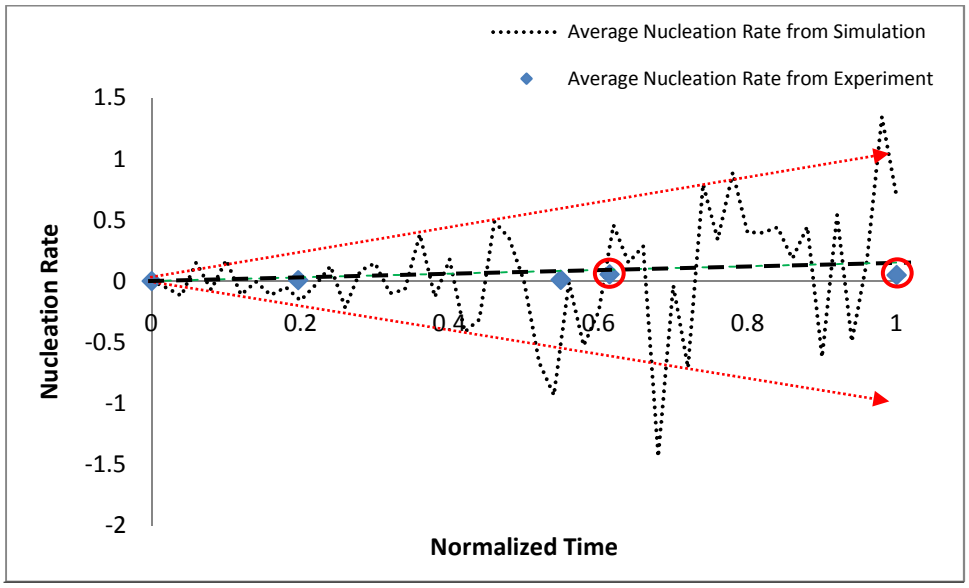

Figure 22. Predicted nucleation rate of double damages by using Brownian motion ($l_e = 50, \Delta t = 0.1, r = 50, \beta = 1$)

It is observed that the Brownian motion with smaller time increments (Figures 19-20) estimates nucleation rate better than larger time increments (Figures 21-22) for double damages. Time increments $\Delta t = 0.01$ in Figure 21 and $\Delta t = 0.1$ in Figure 22 show over prediction of nucleation rate though the variance includes experimental observations of nucleation rate.

Now, the number density of double damages (N_{t_D}) is predicted by using the proposed FBSDE in equation (22-23). For the predefined set of parameters, the predicted number density of double damage is shown in Figures (23-26):

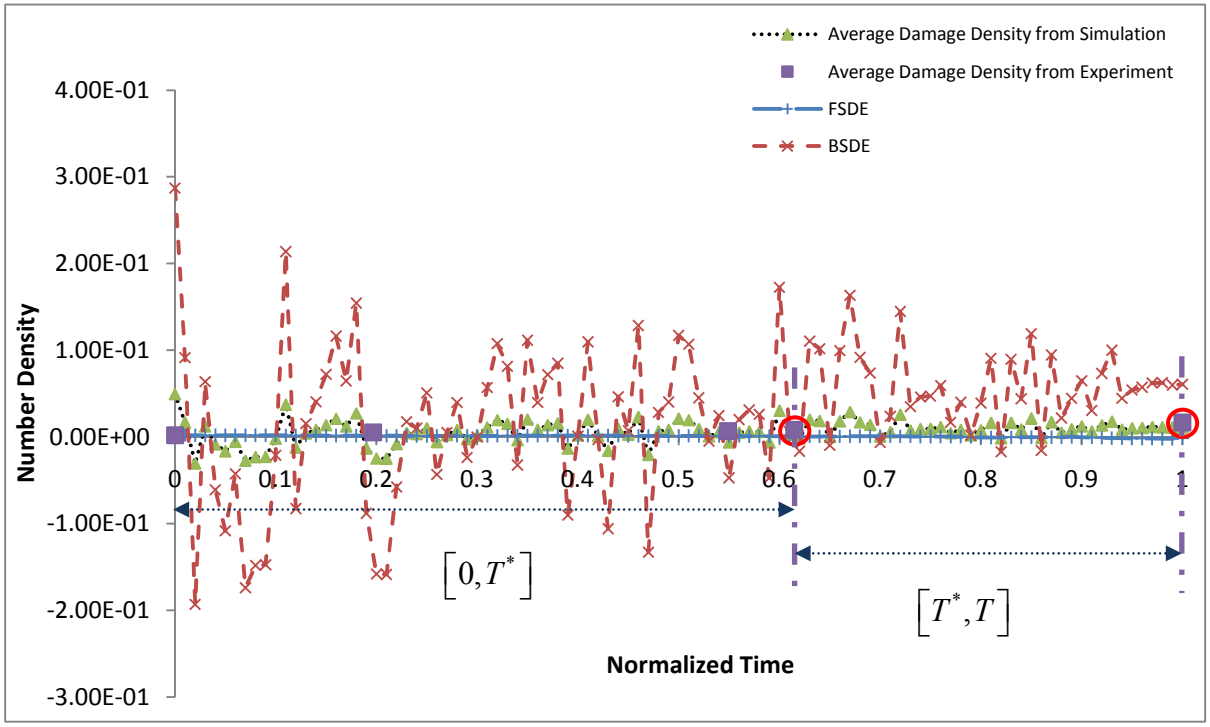

Figure 23. Predicted number density of double damages by using Brownian motion ($l_e = 100, \Delta t = 0.002, r = 100, \beta = 1, \sigma = 1$)

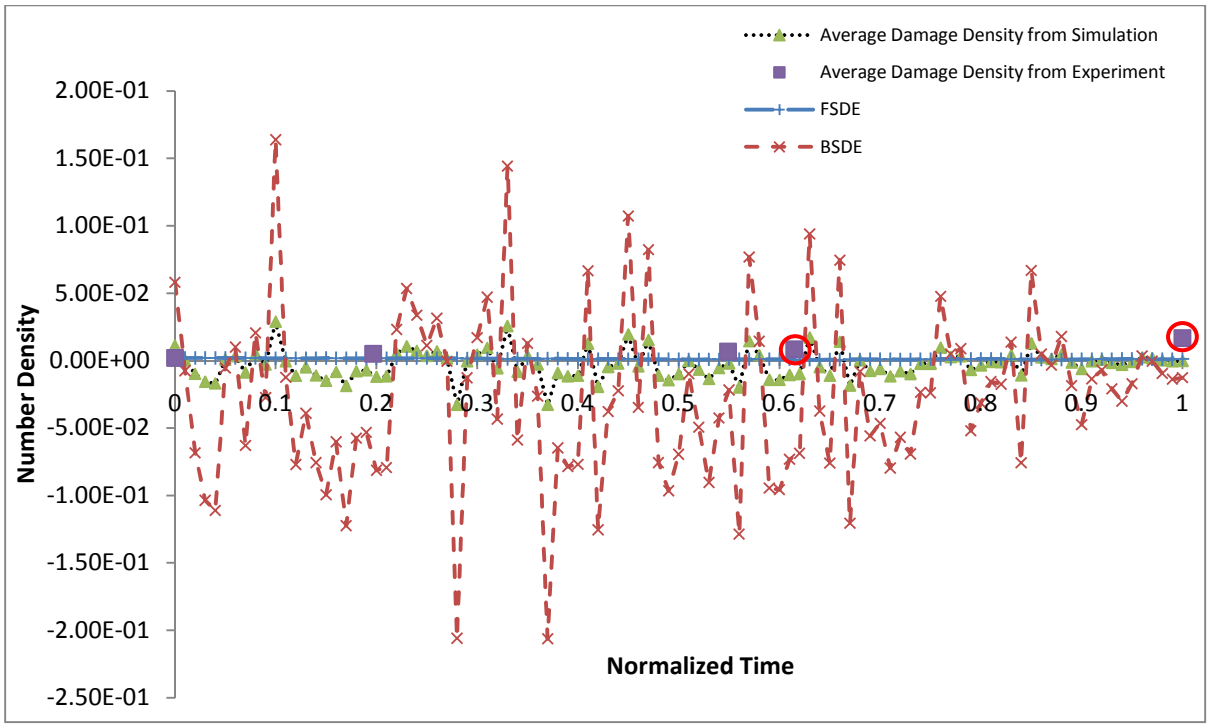

Figure 24. Predicted number density of double damages by using Brownian motion ($l_e = 100, \Delta t = 0.0015, r = 100, \beta = 1, \sigma = 1$)

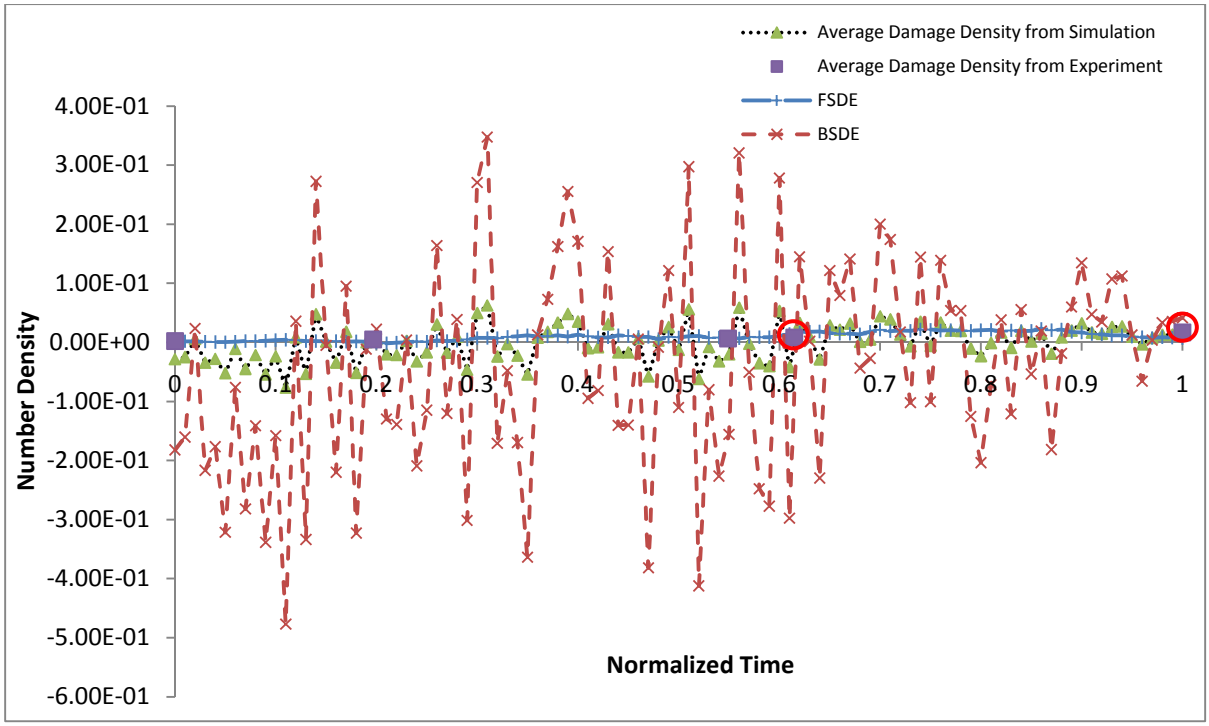

Figure 25. Predicted number density of double damages by using Brownian motion ($l_e = 100, \Delta t = 0.01, r = 100, \beta = 1, \sigma = 1$)

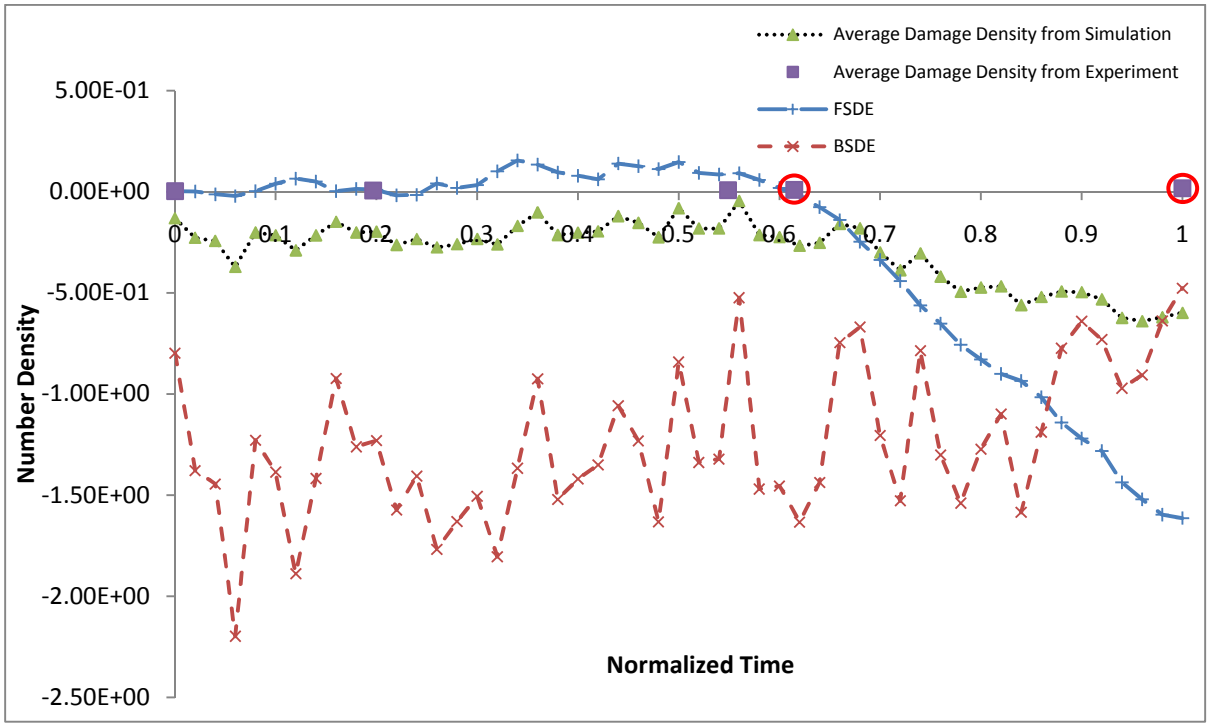

Figure 26. Predicted number density of double damages by using Brownian motion ($l_e = 50, \Delta t = 0.1, r = 50, \beta = 1, \sigma = 1$)

The predicted number density of double damages (N_{t_D}) for $l_e = 100, \Delta t = 0.002, r = 100, \beta = 1, \sigma = 1$ (Figure 23) is quite consistent with the experiment. Although prediction from BSDE is seen to be quite erratic which is also observed in the case for single damages. However, the prediction for $l_e = 100, \Delta t = 0.01, r = 100, \beta = 1, \sigma = 1$ in (Figure 25) is seen to be quite similar to Figure 23. Hence it is consistent with the experiment. It is interesting to observe Figure 26 where the FSDE has an unusual jump in the later portion of time interval. This may happen due to incompatibility of the set of parameters: $l_e = 50, \Delta t = 0.1, r = 50, \beta = 1, \sigma = 1$ with the experimental observation.

It is clearly seen in Figures 24-26 that the prediction for nucleation rate as well as number density of damages are not consistent with the experimental observation.

The results of this study indicate that it is very important to select appropriate set of parameters in order to obtain meaningful and consistent prediction. However, the set of predefined parameters did not focus on the volatility of the Brownian motion in BSDE (σ). As a result simulation is done in order to reduce the erratic behavior in the solution from BSDE with $\sigma = 0.7$. The predictions are in Figures 27-28:

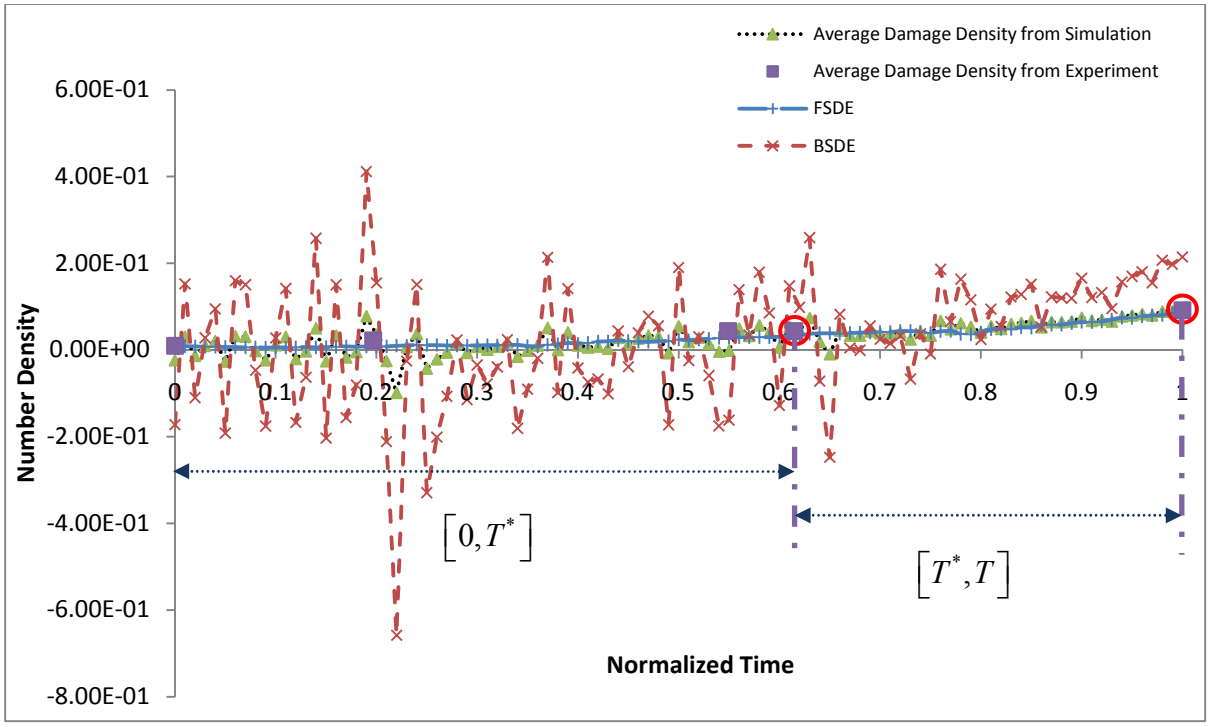

Figure 27. Predicted number density of single damages by using Brownian motion ($l_e = 100, \Delta t = 0.01, r = 100, \beta = 1, \sigma = 0.7$)

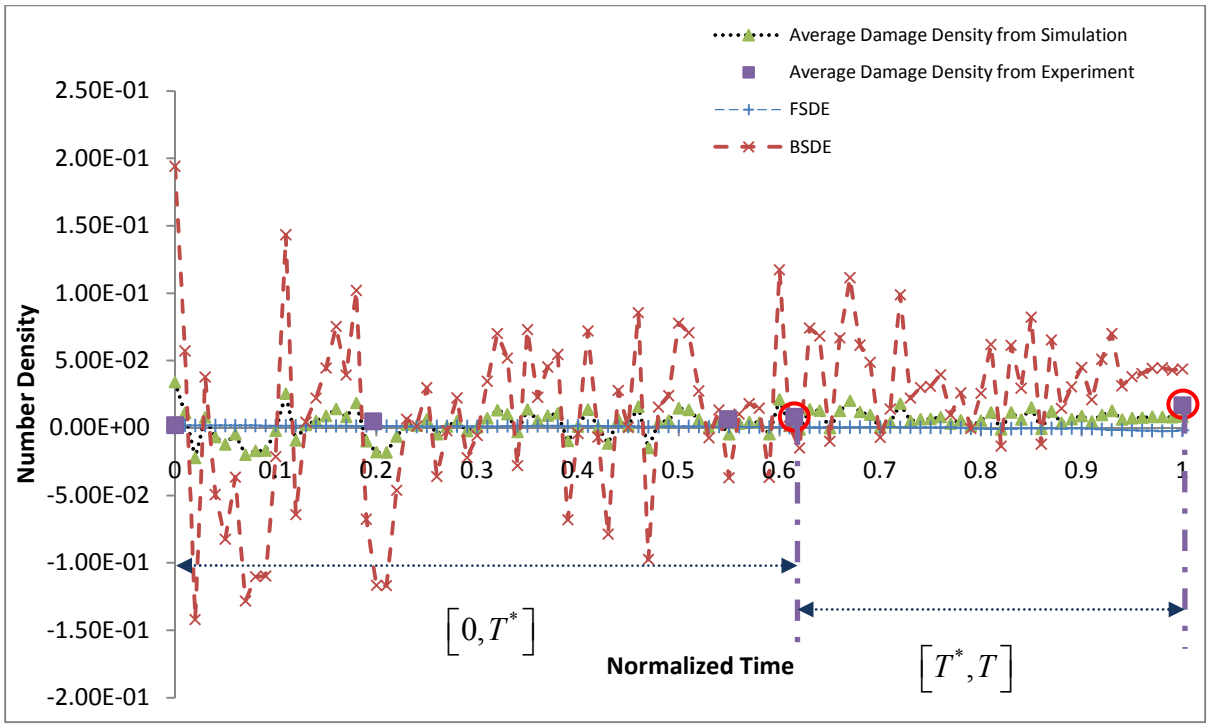

Figure 28. Predicted number density of double damages by using Brownian motion ($l_e = 100, \Delta t = 0.002, r = 100, \beta = 1, \sigma = 0.7$)

In both of the cases (Figures (27-28)), the BSDE possesses reduced fluctuation but the accuracy of the prediction remains same as the case for $\sigma = 1$. Hence we recommend the following set of parameters to be used in numerical simulation scheme for the appropriate prediction of single and double damages:

Single Damages: $l_e = 100, \Delta t = 0.01, r = 100, \beta = 1, \sigma = 0.7$

Double Damages: $l_e = 100, \Delta t = 0.002, r = 100, \beta = 1, \sigma = 0.7$

CHAPTER 6

DISCUSSIONS

In this section we are going to discuss about some issues that are directly influencing the number density prediction. The prediction of number density of micro-damage is subjective to the size of a single block and accounts for only number density evolution due to matrix micro-damages. Although in long run such size effects of the block will be compensated by the individual size of micro-damages. For simplicity, fiber breaking and delamination were not considered in the proposed model.

As mentioned earlier, each image was divided into 6x8 blocks. This was done based on the convenience in damage counting. We were able to capture comparatively smaller damages using this configuration. However, the nucleation rate and number density from experimental observation depends on the configuration chosen to divide each image into sub-regions or blocks. Increased block size may account larger damage as single damage and similarly smaller block size may consider single damage as double damage. In this work we have not addressed the correlation between different length scales of blocks. This is recommended for the future work.

During the damage inspection under optical microscope, it was sometimes difficult to focus uniformly throughout the edge of the specimens. This is mostly due to unpolished edge focused after each individual aging segment. It is also observed in Figure 7(a) and 7(b) that damage ratios $c_S(t), c_D(t)$ are maximum (=1) around 50% of the total time and then start decreasing. One possible reason may be the single damages gradually become double damages and double damages become triple damages. This may cause the decrease in

damage ratio in the second half of the time interval. Moisture swelling is also suspected for this issue, however, it needs more experimental investigation.

ASTM standard (E 112) on average grain size measurement was reviewed for estimating the micro-damage observation strategy. It is to be noted that similar ASTM standard for composite micro-damage measurement is not currently available. Although the methodology adopted in quantifying number density in our case is almost similar to the method described in ASTM E112.

Finally, it is concluded that the current work is mainly focusing on validating the proposed mathematical model with limited experimental data. As a first step a simplest approach is chosen in order to establish the applicability of the proposed model in predicting nucleation rate and number density of damages. A thorough experimental investigation is required to make the model more robust in predicting number density.

CHAPTER 7

CONCLUSIONS

The fundamental concept in this work explores the random feature of micro-crack nucleation/annihilation rates in composites due to environmental ageing. This work is built up on defining these two parameters as random variables following a proper mathematical methodology. We have proposed a theoretical model to predict damage evolution in composite materials under the synergistic effects of various environmental ageing parameters. The model is based on formulation of a generalized Forward- Backward Stochastic Differential Equation (FBSDE) with different environmental ageing parameters such as moisture, temperature, factors related to softening and hardening mechanisms, crack densities, crack length, crack velocities, nucleation and annihilation rates. The micro-crack nucleation or annihilation rates are considered as a continuous random walk model such as "Brownian Motions (BM)" which has been incorporated in the proposed FBSDE. Such randomness in damage nucleation and annihilation process is significantly important particularly under synergistic environmental ageing process in composites. Finally, an experimental validation is carried out which also works as an input to the FBSDE. Using the primary information from first few experimental observations within a limited time, the numerical solution of the proposed FBSDE is shown to predict the nucleation rate as well as number density of single and double damages in an extended time interval. During the environmental degradation a cyclic condition is imposed in order to accelerate the

environmental degradation. Finally, a rigorous investigation was carried out in order to extract the most useful sets of parameters related to FBSDE for the accuracy of the model.

REFERENCES

Augusti, G and Mariano, P.M. (1999). Stochastic Evolution of Microcracks in Continua, *Computer Methods in Applied Mechanics and Engineering,* 168: 155-171.

Bai, Y. Fujiu, K. and Mengfen, X. (1991). Formulation of Statistical Evolution of Microcracks in Solids. *Acta Mechanica Sinica*, 7(1), 59-66.

Bai, Y ,Han, W and Bai, J. (1996). A Statistical Evolution Equation of Microdamage and its Application. *Applications of Continuum Damage Mechanics to Fatigue and Fracture*; Orlando, Florida; USA; May 21, 1996.

Brinson H. F., Morris D. H. and Yeow Y. T. (1978). A new experimental method for the accelerated characterization of composite materials, (Verein Deutscher Ingenieure, *Internationale Konferenz ueber experimentelle Spannungsanalyse*. 6th, presented at Munich, West Germany, Sept. 18-22, 1978.) VDI-Berichte, 313: 395-400.

Case, S. W. and Reifsnider, K. L. (1996). Micromechanical Analysis of Fiber Fracture in Unidirectional Composite Materials, *International Journal of Solids and Structures* (UK), 33(26), 3795-3812.

Chaim R., Baum L. and Brandon D. G. (1989). Mechanical Properties and Microstructure of Whisker-Reinforced Alumina–30 vol% Glass Matrix Composite. *Journal of the American Ceramic Society*, 72(9), 1636-1642.

Collings. T.A and Stone. D.E.W. (1985). Hygrothermal Effects in CFC Laminates: Damaging Effect of Moisture, Temperature and Thermal Spiking. Composite Structures. 3: 341-378.

Huang, Kersen (1987). *StatisticalMechanics*(2nd ed.). New York, NY: John Wiley and Sons.

Iacus M. Stefano. (2008). *Simulation and Inference for Stochastic Differential Equations* (1st ed.). New York, NY: Springer.

Judd, N.C.W. and Wright, W.W. (1978). Voids and Their Effects on Mechanical Properties of Composites- An Appraisal, *SAMPE Journal,* 14, 10-14.

Klebaner Fima C. (2005). *Introduction to Stochastic Calculus with Applications*. London: Imperial College Press.

Li Q, He Ziru, Seng M. S. and Teng A. (1996). Nonequilibrium statistical theory of damage and fracture for glassy polymers, 1. The statistical distribution and evolution of microcracks in glassy polymers, Macromolecular Theory and Simulations, 5(2), 183-197.

Lundgren, Jan-Erik. and Gudmundson, Peter. (1999). Moisture Absorbs ion in Glass-Fiber/Epoxy Laminates with Transverse matrix Cracks, *Composites Science and Technology,* 59, 1983-1991.

Ma. Jin, Yong. Jiongmin. (2007). *Forward-Backward Stochastic Differential Equations and their Applications (Lecture Notes in Mathematics)* (2nd ed.). Springer.

Oksendal. Bernt K. (2002). *Stochastic Differential Equation: An Introduction with Applications* (5th ed.). Springer.

Oliveira, B. F. and Creus, G., J. (2004). An Analytical-Numerical Framework for the Study of Ageing in Fiber Reinforced Polymer Composites, *Composite Structures*, 65(3-4), 443-457.

Papenfuss C, Van P. and Muschik W. (2002). Mesocscopic theory of microcracks. *Arxiv preprint condensed material.*

Reynolds, Tom G. and. McManus, Hugh L. (1999). Accelerated Tests of Environmental Degradation in Composite Materials. *Composite Structures: Theory and Practice*, ASTM STP 1383, P. Grant and C.Q. Rousseau, Eds., American Society for Testing and Materials, West Conshohocken, PA, 2000: 513-525.

Reynolds. Tom. George. (1998). Accelerated Tests of Environmental Degradation in Composite Materials. Thesis. Massachusetts Institute of Technology (MIT).

Roy, S., Xu . Weiqun. Patel, Sneha. And Case, Scott. (2001). Modeling of Moisture Diffusion in the Presence of Bi-axial Damage in Polymer Matrix Composite Laminates, *International Journal of Solids and Structures*, 38: 7627-7641.

Sidney I. Resnick. (1992). *Adventures in Stochastic Processes*. Boston: Birkhauser.

Sobczyk, Kazimierz. (1991). *Stochastic Differential Equations with Applications to Physics and Engineering*. Kluwer Academic Publishes.

Talreja, R. (1985). A Continuum Mechanics Characterization of Damage in Composite Materials, *Proceeding of Royal Society of London. Series A, Mathematical and Physical Sciences,* 399(1817), 195-216.

Talreja, R. (1986). Stiffness Properties of Composite Laminates with Matrix Cracking and Interior Delamination, *Engineering Fracture Mechanics,* 25(5-6), 751-762.

Talreja , R. (1990). Internal Variable Damage Mechanics of Composite Materials, In: Boehler , J.P (Ed.), *Yielding, damage and failure of Anisotropic Solids, EGF* 5, 509-533.

Talreja , R. (1994). Damage Characterization by Internal variables. In: Talreja, R. (Ed.), *Damage Mechanics of Composite Materials,* 53-78.

Varna, J., Joeff, R., Akshantala, .N.V., and Talreja, R. (1999). Damage in Composite laminates with Off-axis plies, *Composites Science and Technology,* 59, 2139-2147.

Yu, Qiao. and Youshi, Hong. (1997). A Theoretical Analysis on Stochastic Behavior of Short Cracks and Fatigue Damage of Metals, *ACTA MECHANICA SOLIDA SINICA,* 10 (4), 352-358.

APPENDIX

Formation of FSDE:

We can recall from equation (2), the generalized damage number density evolution equation can be written as from Liouville's equation:

$$\frac{dn}{dt} = \frac{\partial n}{\partial t} + \frac{\partial(\mathrm{V}_1 n)}{\partial x_1} + \frac{\partial(\mathrm{V}_2 n)}{\partial x_2} + \frac{\partial(\mathrm{V}_3 n)}{\partial x_3} + \frac{\partial(An)}{\partial c} + \frac{\partial(\Xi n)}{\partial \xi} + \frac{\partial(\varphi n)}{\partial \mu} + \frac{\partial(Hn)}{\partial h} + \frac{\partial(\theta n)}{\partial \Phi} = n_N - n_A$$

In an infinitesimal phase space $d\Psi : \langle dt, dx_1, dx_2, dx_3, dc, d\xi, d\mu, dh, d\Phi \rangle$ the infinitesimal change in number density of damage can be written in terms of total differential:

$$dn_t = \frac{\partial n_t}{\partial t} dt + \frac{\partial n_t}{\partial x_i} dx_i + \frac{\partial n_t}{\partial \xi} d\xi + \frac{\partial n_t}{\partial c} dc + \frac{\partial n_t}{\partial \mu} d\mu + \frac{\partial n_t}{\partial h} dh + \frac{\partial n_t}{\partial \Phi} d\Phi \quad \text{(A.1)}$$

Where,

$\frac{\partial n}{\partial x_i} dx_i$ stands for $\sum_{i=1}^{i=3} \frac{\partial n}{\partial x_i} dx_i$

Hence, we can deduce further,

$$dn_t = \left(\frac{\partial n_t}{\partial t} + (\overline{\mathrm{V}} \cdot \nabla) n_t + A \frac{\partial n_t}{\partial c} + \Xi \frac{\partial n}{\partial \xi} + \varphi \frac{\partial n_t}{\partial \mu} + H \frac{\partial n_t}{\partial h} + \theta \frac{\partial n_t}{\partial \Phi} \right) dt \quad \text{(A.2)}$$

After multiplying the equation (9) by dt we can deduce the FSDE i.e. Ito's form:

$$\left(\frac{\partial n_t}{\partial t}+(\overline{\nabla}\cdot\nabla)n_t+A\frac{\partial n_t}{\partial c}+\Xi\frac{\partial n_t}{\partial \xi}+\varphi\frac{\partial n_t}{\partial \mu}+H\frac{\partial n_t}{\partial h}+\theta\frac{\partial n_t}{\partial \Phi}\right)dt=f(n_t,x_1,x_2,x_3,c,\xi,\mu,h,\Phi)dt + \left(n_{N_t}-n_{A_t}\right)dt$$

$$dn_t=f(n_t,x_1,x_2,x_3,c,\xi,\mu,h,\Phi)dt+\left(n_{N_t}-n_{A_t}\right)dt \tag{A.3}$$

Equation (A.3) is the generalized number density evolution equation in a form of FSDE. This FSDE for any $t\in T$ can be written more explicitly by defining the nucleation ra te (see Equation 9):

$$\begin{aligned} dn_t &= f(n_t,t,x_i,c,\xi,\mu,h,\Phi)dt+L(t)dt+\beta B_t dt \\ n_{t_0} &= g(t_0) \end{aligned} \tag{A.4}$$

Formation of BSDE:

The FSDE is formed in order to predict further number density of damages based on given initial condition. However, the FSDE predicts number density of damages blindly because the Brownian motion at any probability state ω does not ensure completely accurate prediction. Hence, it is required to attenuate the result by using BSDE. At every time t, the BSDE is formed based on the result from FSDE and experimental observation (see equations 17-18):

$$-d\overline{n_t} = \sqrt{\left|n_t - \underline{n}_t\right|}dt + \sigma dB_t ; \text{for any } t \in \left[T^*, T\right] \tag{A.5}$$

The term $\sqrt{\left|n_t - \underline{n}_t\right|}$ is used to measure the deviation of number density prediction from FSDE with respect to experimental observation. This term ensures the attenuated overall number density prediction from FBSDE. This term is bounded because:

$$\sqrt{\left|n_t - \underline{n}_t\right|} \le \Lambda$$
$$\Lambda : \text{ Sufficiently large number} \tag{A.6}$$

Finally, the Forward-Backward Stochastic Differential Equation (FBSDE) can be written as:

$$dn_t = f(n_t, t, c, \mu)dt + atdt + \beta B_t dt$$

$$n_{t_0} = \underline{n}_{t_0}$$

$$-d\overline{n_t} = \sqrt{\left|n_t - \underline{n}_t\right|}dt + \sigma dB_t \tag{A.7}$$

$$\overline{n_T} = \underline{n}_{T^*} \approx \underline{n}_T$$